Stable Nonlinear Trilateral Impedance Control for Dual-User Haptic Teleoperation Systems with Communication Delays

Mojtaba Sharifi
Department of Mechanical Engineering, Sharif University of Technology
Azadi St., P.O. Box: 11155-9567, Tehran, Iran
mojtaba_sharifi@mech.sharif.edu

Hassan Salarieh[1]
Department of Mechanical Engineering, Sharif University of Technology
Azadi St., P.O. Box: 11155-9567, Tehran, Iran
salarieh@sharif.edu

Saeed Behzadipour
Department of Mechanical Engineering, Sharif University of Technology
Azadi St., P.O. Box: 11155-9567, Tehran, Iran
behzadipour@sharif.edu

Mahdi Tavakoli
Department of Electrical and Computer Engineering, University of Alberta, Edmonton, Alberta, T6G 1H9 Canada
mahdi.tavakoli@ualberta.ca

ABSTRACT

A new nonlinear adaptive impedance-based trilateral controller is proposed to ensure the absolute stability of multi-DOF dual-user haptic teleoperation systems subjected to communication delays. Using this strategy, reference impedance models are realized for the trilateral teleoperation system represented by a three-port network to facilitate cooperation of two human operators in order to perform a remote physical task. For this purpose, an impedance model defines the desired haptic interaction between the two human operators while another impedance model specifies the desired behavior of the slave robot in terms of tracking the mater robots' trajectories during interaction with the remote environment. It is

[1] Corresponding author.

shown that different performance goals such as position synchronization and force reflection can be achieved via different adjustments to the impedance parameters. The sufficient conditions for the trilateral haptic system's absolute stability are investigated in terms of the impedance models' parameters. Accordingly, guidelines for modification of the impedance parameters are obtained to guarantee the absolute stability of the trilateral haptic system in the presence of communication time delays. A trilateral nonlinear version of the Model Reference Adaptive Impedance Control (MRAIC) scheme is developed for implementing the proposed reference impedance models on the masters and the slave. The convergence of robots' trajectories to desired responses and the robustness against modeling uncertainties are ensured using the proposed controller as proven by the Lyapunov stability theorem. The proposed impedance-based control strategy is evaluated experimentally by employing a nonlinear multi-DOF teleoperated trilateral haptic system with and without communication delays.

1. INTRODUCTION

In recent years, research in the field of haptic teleoperation has moved beyond the bilateral single-master/single-slave systems by introducing multilateral systems with multiple masters and/or slaves. Using multilateral teleoperation systems, operators can cooperatively perform a physical operation by a slave robot in a remote environment. Novel practical applications of these systems include telesurgical training (mentoring a trainee surgeon by an experienced surgeon during tele-surgery operations) [1, 2], robotic tele-rehabilitation [3, 4] and complementary motion teleoperation (sharing the motions of a multi-DOF slave robot in different directions between two master robots (operators) to perform complex tasks) [5]. The control of multilateral systems is an important issue to perform teleoperation tasks successfully with the required stability.

Accordingly, the literature of previous multilateral controllers and the contribution of the proposed strategy are mentioned in the rest of this section.

Different control architectures have been suggested for bilateral single-master/single-slave systems. Among them, many controllers have been designed for 1-DOF linear teleoperation systems [6-10], including the 4-channel control architecture as the most successful one in providing transparency [8, 9]. However, to solve the issue of master and slave modeling uncertainty, adaptive controllers have been suggested for linear teleoperation systems dealt with parametric uncertainties [11, 12].

In order to perform complex tasks in multi-dimensional space, multi-DOF nonlinear telerobotic systems have been studied and utilized instead of 1-DOF linear ones. Accordingly, bilateral adaptive controllers [13, 14] have been presented to provide the stability of uncertain nonlinear teleoperation systems. Also, PD [15] and other adaptive [16-18] control strategies have been suggested for synchronization of the master and slave positions in the presence of time delays. Aimed at both position and force tracking in bilateral multi-DOF systems (i.e., transparency condition), nonlinear adaptive controllers have been extended in [19-21].

In recent years, multilateral (e.g., trilateral) controllers and corresponding stability analyses have been developed for multi-user (e.g., dual-user) teleoperation systems in order to perform cooperative tasks. Lo et al. [22] have investigated a two-channel position–force controller to enable the cooperation of multiple operators by employing multiple robots. A four-channel control architecture has been suggested in [23], which has been implemented on a haptic training system [24].

Robust H_∞ – based [1] and μ – synthesis [25] approaches have been developed for linear multilateral systems, and some adaptive controllers [26, 27] have been also proposed for collaborative training applications using a dual-user haptic system. In these controllers [1, 25, 26], the stability of uncertain teleoperation system has been ensured for a limited range of the human's and environment's dynamic parameters. A six-channel multilateral shared control method [28] has been used to evaluate the kinesthetic performance of a dual-user system. The human operators' performance has been evaluated in [29] for different factors of virtual environment using a dual-user haptic guidance system. Due to the challenges of stability proof for multilateral teleoperation systems, the communication delay has not been considered in the mentioned previous works [23-26, 28, 29] and their stability analyses.

Some other control architectures [30-33] have been suggested based on the passivity criterion for multilateral teleoperation systems, which is more conservative and results in more limiting conditions in comparison with the absolute stability criterion as shown in [34]. Also, a multilateral control method [35] has been proposed and analyzed for the stability using the small-gain theorem, which resulted in bounds on the human operator and the environment dynamics.

In some recent studies [36-38], the third port of a dual-user teleoperation system (modeled as a three-port network) has been assumed to be coupled to a known termination such that the system can be reduced to a two-port network. This assumption may not be met in all practical applications of trilateral haptic systems. As a result of this limiting assumption, stability analyses of bilateral teleoperation systems

(modeled as two-port networks) based on the Llewellyn's criterion [39] for absolute stability have been presented. However, the conditions of absolute stability as an efficient criterion have been recently obtained in [40] for trilateral haptic systems, which is an extension of the Llewellyn's criterion for bilateral systems.

Accordingly, in the present work, a new nonlinear Trilateral Model Reference Adaptive Impedance Controller (TMRAIC) is developed for dual-user multi-DOF haptic systems. This strategy has the following novel characteristics and advantages in comparison with the previous trilateral controllers:

1. New impedance-based trilateral control objectives are defined for the cooperation of two operators to perform a task in the remote environment using a dual-user haptic teleoperation system. For this purpose, a reference impedance model is designed for the master robots that incorporates the forces applied by the two operators and the environment, and dictates the haptic force feedback from the environment and one operator to the other operator. Another reference impedance model is considered for the slave robot, which defines the flexibility of the slave in tracking two masters' position trajectories in response to the environment force. Accordingly, two new impedance models are the control objectives of trilateral system (including three robots) instead of previous position-force based objectives [25-30, 33, 37, 38].
2. In order to implement these impedance models and track their responses by the multi-DOF masters and slave robots, a new nonlinear Trilateral Model Reference Adaptive Impedance Control (TMRAIC) scheme is presented based on the MRAIC method [41] suggested and evaluated recently for a single robot. Since the closed-

loop dynamics of the robot is made similar to the corresponding reference impedance model in the MRAIC, this scheme [41] is more effective than other nonlinear adaptive impedance controllers (such as [42]) in implementing an impedance model for a haptic robot. This strategy (MRAIC) is extended for nonlinear trilateral teleoperation systems (including 3 robots) in the current work with two new cooperative impedance objectives (described in above item 1).

3. The absolute stability of the trilateral haptic system is proven using the criterion obtained recently in [40] for three-port networks, without assuming any reduction to a two-port network through coupling the third port to a known termination (like [36-38]). The possibility of absolute stability proof (without any reduction to a two-port network) is due to the trilateral impedance control (TMRAIC) that is described in the above items 1 and 2. Based on the obtained conditions for the trilateral absolute stability, the required adjustments for the impedance parameters are investigated in terms of bounds on the communication delays. In other words, using appropriate parameters in the reference impedance models, the trilateral haptic system becomes robust against time delays. In addition, a Lyapunov stability analysis is employed to prove the tracking convergence of the masters and slave trajectories to their corresponding desired responses in the presence of modeling uncertainties. Therefore, the absolute stability and Lyapunov stability criteria are combined in this work to guarantee the robustness and tracking convergence of the proposed trilateral teleoperation system in the presence of communication delay and dynamics uncertainties.

4. As another feature of the proposed method, desirable performances of the dual-user haptic system can be achieved using appropriate adjustments to the impedance models. In a case of impedance adjustment, the trilateral position synchronization and force reflection objectives can be provided (as the transparent case of teleoperation). Guidelines for impedance parameters adjustment to achieve transparency and absolute stability are also presented.

2. Nonlinear Dynamics of Trilateral Haptic Systems

The nonlinear model of a trilateral multi-DOF haptic system including two master and one slave robots interacting with two human operators and a remote environment, respectively, is defined in the Cartesian space as [43, 44]:

$$\mathbf{M}_{\mathbf{x},m_1}(\mathbf{q}_{m_1})\ddot{\mathbf{x}}_{m_1}+\mathbf{C}_{\mathbf{x},m_1}(\mathbf{q}_{m_1},\dot{\mathbf{q}}_{m_1})\dot{\mathbf{x}}_{m_1}+\mathbf{G}_{\mathbf{x},m_1}(\mathbf{q}_{m_1})+\mathbf{F}_{\mathbf{x},m_1}(\dot{\mathbf{q}}_{m_1})=\mathbf{f}_{m_1}+\mathbf{f}_{hum_1} \quad (1)$$

$$\mathbf{M}_{\mathbf{x},m_2}(\mathbf{q}_{m_2})\ddot{\mathbf{x}}_{m_2}+\mathbf{C}_{\mathbf{x},m_2}(\mathbf{q}_{m_2},\dot{\mathbf{q}}_{m_2})\dot{\mathbf{x}}_{m_2}+\mathbf{G}_{\mathbf{x},m_2}(\mathbf{q}_{m_2})+\mathbf{F}_{\mathbf{x},m_2}(\dot{\mathbf{q}}_{m_2})=\mathbf{f}_{m_2}+\mathbf{f}_{hum_2} \quad (2)$$

$$\mathbf{M}_{\mathbf{x},s}(\mathbf{q}_s)\ddot{\mathbf{x}}_s+\mathbf{C}_{\mathbf{x},s}(\mathbf{q}_s,\dot{\mathbf{q}}_s)\dot{\mathbf{x}}_s+\mathbf{G}_{\mathbf{x},s}(\mathbf{q}_s)+\mathbf{F}_{\mathbf{x},s}(\dot{\mathbf{q}}_s)=\mathbf{f}_s-\mathbf{f}_{env} \quad (3)$$

where indices m_1, m_1 and s correspond to master 1, master 2 and the slave robots. $\mathbf{q}_{m_1}$, $\mathbf{q}_{m_2}$ and $\mathbf{q}_s$ are the joint positions, $\mathbf{x}_{m_1}$, $\mathbf{x}_{m_2}$ and $\mathbf{x}_s$ are the Cartesian positions, $\mathbf{M}_{\mathbf{x},m_1}(\mathbf{q}_{m_1})$, $\mathbf{M}_{\mathbf{x},m_2}(\mathbf{q}_{m_2})$ and $\mathbf{M}_{\mathbf{x},s}(\mathbf{q}_s)$ are the inertia matrices, $\mathbf{C}_{\mathbf{x},m_1}(\mathbf{q}_{m_1},\dot{\mathbf{q}}_{m_1})$, $\mathbf{C}_{\mathbf{x},m_2}(\mathbf{q}_{m_2},\dot{\mathbf{q}}_{m_2})$ and $\mathbf{C}_{\mathbf{x},s}(\mathbf{q}_s,\dot{\mathbf{q}}_s)$ represent the Coriolis and centrifugal terms, $\mathbf{G}_{\mathbf{x},m_1}(\mathbf{q}_{m_1})$, $\mathbf{G}_{\mathbf{x},m_2}(\mathbf{q}_{m_2})$ and $\mathbf{G}_{\mathbf{x},s}(\mathbf{q}_s)$ are the gravity terms, $\mathbf{F}_{\mathbf{x},m_1}(\dot{\mathbf{q}}_{m_1})$, $\mathbf{F}_{\mathbf{x},m_2}(\dot{\mathbf{q}}_{m_2})$ and $\mathbf{F}_{\mathbf{q},s}(\dot{\mathbf{q}}_s)$ are the friction forces, and $\mathbf{f}_{m_1}$, $\mathbf{f}_{m_2}$ and $\mathbf{f}_s$ are the input control forces for master 1, master 2 and the slave robots, respectively. Also, $\mathbf{f}_{hum_1}$ and $\mathbf{f}_{hum_2}$ are the interaction forces of the

human operators applied to masters 1 and 2, and $\mathbf{f}_{env}$ is the interaction force that the slave robot applies to the remote environment. The above mentioned dynamic matrices and vectors have these properties [43, 44] (considering $j = m_1, m_2, s$):

Properties. $\mathbf{M}_{\mathbf{x},j}(\mathbf{q}_j)$ is symmetric and positive definite, $\left(\dot{\mathbf{M}}_{\mathbf{x},j}(\mathbf{q}_j) - 2\mathbf{C}_{\mathbf{x},j}(\mathbf{q}_j,\dot{\mathbf{q}}_j)\right)$ is skew symmetric, and the left sides of (1), (2) and (3) can be linearly parameterized as

$$\mathbf{M}_{\mathbf{x},j}(\mathbf{q}_j)\boldsymbol{\xi}_{\mathbf{1},j} + \mathbf{C}_{\mathbf{x},j}(\mathbf{q}_j,\dot{\mathbf{q}}_j)\boldsymbol{\xi}_{\mathbf{2},j} + \mathbf{G}_{\mathbf{x},j}(\mathbf{q}_j) + \mathbf{F}_{\mathbf{x},j}(\dot{\mathbf{q}}_j) = \mathbf{R}_{\mathbf{x},j}(\xi_{1,j},\xi_{2,j},\mathbf{q}_j,\dot{\mathbf{q}}_j)\boldsymbol{\delta}_{\mathbf{x},j} \qquad (4)$$

where $\boldsymbol{\delta}_{\mathbf{x},j}$ is the vector of unknown dynamic parameters of each robot, and $\mathbf{R}_{\mathbf{x},j}$ is the regressor matrix including known functions of the vectors $\xi_{1,j}$ and $\xi_{2,j}$.

2.1. Trilateral Signal Transmission in the Proposed Teleoperation System

The schematic diagram of the trilateral teleoperated haptic system and required transmitted signals for the proposed control method are illustrated in Fig. 1. The bounded time delays T_1 and T_2 are considered in the communication channels between the master console (operators' site) and the slave console (environment site). As shown in Fig.1, the combination of operators forces ($\mathbf{f}_{hum_1}$ and $\mathbf{f}_{hum_2}$) and the transmitted environment forces ($\mathbf{f}_{env}^{d}$) are used in the master impedance model to obtain the desired masters trajectory $\mathbf{x}_{imp_m}$. This trajectory is tracked by the master robots 1 and 2 using their nonlinear MRAIC controllers. The position data of two master robots or operators ($\mathbf{x}_{m_1}^{d}$ and $\mathbf{x}_{m_2}^{d}$) are also transmitted to the slave console to obtain the desired slave trajectory $\mathbf{x}_{imp_s}$ as a response of the slave impedance model. The slave robot should also track the response of this impedance model using its MRAIC controller. The

structures of impedance models and the trilateral controller are described in Sec. 3 and 4, respectively.

The transmitted input and output signals via the communication channels (Fig. 1) have the following relation:

$$\mathbf{x}^d_{m_1}(t) = \mathbf{x}_{m_1}(t - T_1),\ \mathbf{x}^d_{m_2}(t) = \mathbf{x}_{m_2}(t - T_1),\ \mathbf{f}^d_{env}(t) = \mathbf{f}_{env}(t - T_2) \tag{5}$$

Note that the time delays (T_1, T_2) of real communication channels are usually close to constant and do not change very much during a teleoperation task and an upper bound of delay can be considered as the worst case for them. However, if the communication delays are considerably time-varying, they can be measured online based on the sending and receiving times of transmitted signals as proposed in [45]. Therefore, the varying portion of communication delays can be obtained [45] and then compensated [46] such that the upper bound of delay in each channel is treated as a permanent constant delay for absolute stability analysis, as considered in this work. The basis of delay compensation is introduced in [46] by modeling a time-varying delay in the communication channel as a constant value together with an external disturbance that can be estimated.

The positions and haptic forces are scaled between the masters and the slave robots (due to the application of teleoperation system) using scaling factors η_{x} and η_{f} :

$$\mathbf{x}^d_{m_1 scaled} = \eta_{\mathrm{x}}\, \mathbf{x}^d_{m_1},\ \ \mathbf{x}^d_{m_2 scaled} = \eta_{\mathrm{x}}\, \mathbf{x}^d_{m_2},\ \ \mathbf{f}^d_{env_{scaled}} = \eta_{\mathrm{f}}\, \mathbf{f}^d_{env} \tag{6}$$

These scaled position and forces are utilized in the control objectives presented in the next section.

3. TRILATERAL IMPEDANCE-BASED CONTROL OBJECTIVES

3.1. Master Reference Impedance Model: For Cooperative Haptic Force Perception

The first reference impedance model is defined for the two master robots such that each operator perceives the other operator force and also the environment force applied to the slave robot. Accordingly, the inputs of this impedance model (as a desired dynamics) are the human operators' forces $\mathbf{f}_{hum_1}$ and $\mathbf{f}_{hum_2}$ and the transmitted environment force $\mathbf{f}_{env}^{d}$, and its output is the desired masters' trajectory $\mathbf{x}_{imp_m}$ as

$$m_{imp_m}\ddot{\mathbf{x}}_{imp_m} + b_{imp_m}\dot{\mathbf{x}}_{imp_m} = \alpha_{\mathrm{f}}\mathbf{f}_{hum_1} + (1-\alpha_{\mathrm{f}})\mathbf{f}_{hum_2} - \eta_{\mathrm{f}}\,\mathbf{f}_{env}^{d} \tag{7}$$

where $\mathbf{x}_{imp_m}$ is the position response of this reference impedance model, and the force authority factor $0 \le \alpha_{\mathrm{f}} \le 1$ specifies the haptic force authority of operators with respect to each other. Using $\alpha_{\mathrm{f}} = 0.5$, operators 1 and 2 have the same authority to affect the desired master impedance response $\mathbf{x}_{imp_m}$ based on (7). Also, employing $\alpha_{\mathrm{f}} > 0.5$ or $\alpha_{\mathrm{f}} < 0.5$ the authority of Operator 1 becomes higher or lower than that of Operator 2, respectively. m_{imp_m} and b_{imp_m} in (7) are the desired virtual mass and damping parameters of the master reference impedance model, respectively. When the master robots achieve their control objective, which is tracking the response of the master reference model (7) ($\mathbf{x}_{m_1} \to \mathbf{x}_{imp_m}$ and $\mathbf{x}_{m_2} \to \mathbf{x}_{imp_m}$), each operator senses the interaction forces of the other operator and the environment and also the mass m_{imp_m} and damping b_{imp_m} elements. Note that a stiffness parameter is not used in the impedance model (7) such that the force reflection performance can be achieved at every arbitrary position,

i.e., $(\alpha_{\mathrm{f}}\mathbf{f}_{hum_1} + (1-\alpha_{\mathrm{f}})\mathbf{f}_{hum_2} - \eta_{\mathrm{f}}\,\mathbf{f}_{env}^{d}) \to 0$ as will be described in Sec. 3.3. If a stiffness element $k_{imp_m}(\mathbf{x}_{imp_m} - \mathbf{x}_0)$ was considered at the left side of (7), when the impedance response $\mathbf{x}_{imp_m}$ takes a distance from the origin $\mathbf{x}_0$, a nonzero steady-state force error will be obtained from the right side of (7), i.e., $(\alpha_{\mathrm{f}}\mathbf{f}_{hum_1} + (1-\alpha_{\mathrm{f}})\mathbf{f}_{hum_2} - \eta_{\mathrm{f}}\,\mathbf{f}_{env}^{d}) \neq 0$, which is not desirable for the transparency condition.

3.2. Slave Reference Impedance Model: For Position Synchronization

Another reference impedance model is defined for the slave robot as the desired dynamics between the remote environment force $\mathbf{f}_{env}$ (as the input) and the slave robot' deviation $\tilde{\mathbf{x}}_{imp_s}$ from a linear combination of the master robots' trajectories (as the output):

$$m_{imp_s}\ddot{\tilde{\mathbf{x}}}_{imp_s} + b_{imp_s}\dot{\tilde{\mathbf{x}}}_{imp_s} + k_{imp_s}\tilde{\mathbf{x}}_{imp_s} = -\mathbf{f}_{env} \tag{8}$$

Here,

$$\tilde{\mathbf{x}}_{imp_s} = \mathbf{x}_{imp_s} - \eta_{\mathrm{x}}\,(\alpha_{\mathrm{x}}\mathbf{x}_{m_1}^{d} + (1-\alpha_{\mathrm{x}})\mathbf{x}_{m_2}^{d}) \tag{9}$$

where $0 \le \alpha_{\mathrm{x}} \le 1$ is the position dominance factor. Since master 1 (or operator 1) and master 2 (or operator 2) will track the same desired trajectory (that is the master impedance response $\mathbf{x}_{imp_m}$), the value of α_{x} does not considerably affect the linear combination $(\alpha_{\mathrm{x}}\mathbf{x}_{m_1} + (1-\alpha_{\mathrm{x}})\mathbf{x}_{m_2})$ in Eq. (9). m_{imp_s}, b_{imp_s} and k_{imp_s} are the desired virtual mass, damping, and stiffness parameters of the slave reference impedance model (8) that specify the level of the slave robot's flexibility $\tilde{\mathbf{x}}_{imp_s}$ with respect to the masters' trajectories in response to the environment force $\mathbf{f}_{env}$.

The parameters of master (7) and slave (8) impedance models should be adjusted appropriately based on the required characteristics of the teleoperation system and the stability analysis. The appropriate impedance adjustment for the transparent case of tele-haptic system is described in Sec. 3.3, and the required modifications of the impedance parameters to ensure the trilateral absolute stability in the presence of communication delays are presented in Sec. 5.

3.3. Impedance Adjustment for Trilateral Position Synchronization and Force Reflection (Transparency)

The two employed reference impedance models (7) and (8) can be adjusted such that the position synchronization and force reflection objectives are achieved in the trilateral haptic system. For the purpose of force reflection, small values should be considered for the parameters m_{imp_m} and b_{imp_m} in the master reference impedance model (7). In this case, due to the boundedness of $\dot{\mathbf{x}}_{imp_m}$ and $\ddot{\mathbf{x}}_{imp_m}$, the left side of (7) is small. Therefore, the right side of (7) also becomes small, i.e., $(\alpha_{\mathrm{f}}\mathbf{f}_{hum_1} + (1-\alpha_{\mathrm{f}})\mathbf{f}_{hum_1} - \eta_{\mathrm{f}}\,\mathbf{f}_{env}^{d}) \approx 0$, which provides the cooperative force reflection performance in the trilateral teleoperation case. In other words, the environment interaction force is sensed and shared between two operators such that the combination of operators' forces converges to the scaled environment force:

$$\alpha_{\mathrm{f}}\mathbf{f}_{hum_1} + (1-\alpha_{\mathrm{f}})\mathbf{f}_{hum_2} \rightarrow \eta_{\mathrm{f}}\,\mathbf{f}_{env}^{d} \qquad (10)$$

Thus, operators 1 and 2 have a haptic cooperation in performing a remote task and applying forces to the task environment.

Also, in order to have a position synchronization performance, large values should be employed for the parameters m_{imp_s}, b_{imp_s} and k_{imp_s} in the slave reference impedance model (8). Given the boundedness of $-\mathbf{f}_{env}$ in the right side of (8), the terms $\tilde{\mathbf{x}}_{imp_s}$, $\dot{\tilde{\mathbf{x}}}_{imp_s}$, $\ddot{\tilde{\mathbf{x}}}_{imp_s}$ in the left side of (8) become small under large slave impedance parameters m_{imp_s}, b_{imp_s} and k_{imp_s}. Therefore, the desired position tracking error becomes small ($\tilde{\mathbf{x}}_{imp_s} \to 0$) using this impedance adjustment, and the trilateral position synchronization is achieved based on Eq. (9) as

$$\mathbf{x}_{imp_s} \to \eta_{\mathrm{x}} (\alpha_{\mathrm{x}} \mathbf{x}_{m_1}^d + (1-\alpha_{\mathrm{x}}) \mathbf{x}_{m_2}^d) \tag{11}$$

This means that the slave robot tracks the trajectory of the master robots (i.e., the operators). Note that simultaneous position synchronization and force reflection performances can be achieved using the above-mentioned impedance adjustments, which provide a trilateral transparency condition for the telerobotic system.

4. NONLINEAR TRILATERAL MODEL REFERENCE ADAPTIVE CONTROL

The schematic block diagram of the proposed nonlinear trilateral model reference adaptive impedance controller (TMRAIC) is shown in Fig. 2. As introduced in Sec. 3, two reference impedance models (7) and (8) are defined for the dual-user tele-haptic system. The dynamic models of two masters and the slave robots are allowed to have parametric uncertainties. Note that the dynamic models of the human operators and the remote environment are not required due to the direct measurement of their applied interaction forces ($\mathbf{f}_{hum_1}$, $\mathbf{f}_{hum_2}$ and $\mathbf{f}_{env}$) using three force sensors.

4.1. Controller Design

The nonlinear trilateral control laws of the masters and the slave are designed based on the nonlinear Model Reference Adaptive Impedance control (MRAIC) scheme suggested recently in [41] for the physical interaction with one robot. In this method, the robot's closed-loop dynamics is made similar to the reference impedance model. It has been shown in [41] that the MRAIC scheme is more effective than other simple adaptive impedance controllers (such as [42]) in tracking the impedance model response by the robot. The nonlinear trilateral extension of this MRAIC strategy is developed and used in this work by defining two new cooperative impedance objectives (Eqs. (7) and (8)). For this purpose, using positive parameters in the master and slave reference impedance models (7) and (8), the following properties are obtained:

$$m_{imp_m}^{-1} b_{imp_m} > 0 \ , \quad m_{imp_s}^{-1} b_{imp_s} > 0 \ , \quad m_{imp_s}^{-1} k_{imp_s} > 0 \tag{12}$$

In this scheme, the above-mentioned properties of reference models are employed in the controller structure. Accordingly, based on the reference impedance models (7) and (8) and their properties (12), the masters and slave sliding surfaces are defined as

$$\begin{aligned}
\mathbf{s}_{m_1} &= \dot{\tilde{\mathbf{x}}}_{m_1} + \left(m_{imp_m}^{-1} b_{imp_m} \right) \tilde{\mathbf{x}}_{m_1} + \lambda_{2,m_1} \int_0^t \tilde{\mathbf{x}}_{m_1} \, dt \ , \\
\mathbf{s}_{m_2} &= \dot{\tilde{\mathbf{x}}}_{m_2} + \left(m_{imp_m}^{-1} b_{imp_m} \right) \tilde{\mathbf{x}}_{m_2} + \lambda_{2,m_2} \int_0^t \tilde{\mathbf{x}}_{m_2} \, dt \ , \\
\mathbf{s}_s &= \dot{\tilde{\mathbf{x}}}_s + \left(m_{imp_s}^{-1} b_{imp_s} \right) \tilde{\mathbf{x}}_s + \left(m_{imp_s}^{-1} k_{imp_s} \right) \int_0^t \tilde{\mathbf{x}}_s \, dt
\end{aligned} \tag{13}$$

where $m_{imp_m}^{-1} b_{imp_m}$, λ_{2,m_1} , λ_{2,m_2} , $m_{imp_s}^{-1} b_{imp_s}$ and $m_{imp_s}^{-1} k_{imp_s}$ are positive constants.

$\tilde{\mathbf{x}}_{m_1} = \mathbf{x}_{m_1} - \mathbf{x}_{imp_m}$, $\tilde{\mathbf{x}}_{m_2} = \mathbf{x}_{m_2} - \mathbf{x}_{imp_m}$ and $\tilde{\mathbf{x}}_s = \mathbf{x}_s - \mathbf{x}_{imp_s}$ are the master 1, master 2 and slave position tracking errors with respect to responses of the master impedance model

($\mathbf{x}_{imp_m}$) and the slave impedance model ($\mathbf{x}_{imp_s}$), respectively. The reference velocities are also defined for the robots as

$$\begin{aligned}
\dot{\mathbf{x}}_{\mathbf{r},m_1} &= \dot{\mathbf{x}}_{imp_m} - m_{imp_m}^{-1} b_{imp_m} \tilde{\mathbf{x}}_{m_1} - \lambda_{2,m_1} \int_0^t \tilde{\mathbf{x}}_{m_1}\, dt\,, \\
\dot{\mathbf{x}}_{\mathbf{r},m_2} &= \dot{\mathbf{x}}_{m_1} - m_{imp_m}^{-1} b_{imp_m} \tilde{\mathbf{x}}_{m_2} - \lambda_{2,m_2} \int_0^t \tilde{\mathbf{x}}_{m_2}\, dt\,, \\
\dot{\mathbf{x}}_{\mathbf{r},s} &= \dot{\mathbf{x}}_{imp_s} - m_{imp_s}^{-1} b_{imp_s} \tilde{\mathbf{x}}_s - m_{imp_s}^{-1} k_{imp_s} \int_0^t \tilde{\mathbf{x}}_s\, dt
\end{aligned} \tag{14}$$

such that the sliding surfaces (13) are rewritten as $\mathbf{s}_{m_1} = \dot{\mathbf{x}}_{m_1} - \dot{\mathbf{x}}_{\mathbf{r},m_1}$, $\mathbf{s}_{m_2} = \dot{\mathbf{x}}_{m_2} - \dot{\mathbf{x}}_{\mathbf{r},m_2}$ and $\mathbf{s}_s = \dot{\mathbf{x}}_s - \dot{\mathbf{x}}_{\mathbf{r},s}$. Now, the nonlinear trilateral model reference adaptive impedance control (TMRAIC) scheme for the two masters and the slave robots are designed in Cartesian space as

$$\begin{aligned}
\mathbf{f}_{m_1} = \hat{\mathbf{M}}_{\mathbf{x},m_1} & \begin{pmatrix} m_{imp_m}^{-1}\left(\alpha_{\mathrm{f}}\mathbf{f}_{hum_1} + (1-\alpha_{\mathrm{f}})\mathbf{f}_{hum_2} - \eta_{\mathrm{f}}\mathbf{f}_{env}^{d}\right) \\ -m_{imp_m}^{-1} b_{imp_m}\dot{\mathbf{x}}_{m_1} - \lambda_{2,m_1}\tilde{\mathbf{x}}_{m_1} - \lambda_{3,m_1}\mathbf{s}_{m_1} \end{pmatrix} \\
& + \hat{\mathbf{C}}_{\mathbf{x},m_1}\dot{\mathbf{x}}_{\mathbf{r},m_1} + \hat{\mathbf{G}}_{\mathbf{x},m_1} + \hat{\mathbf{F}}_{\mathbf{x},m_1} - \mathbf{f}_{hum_1}
\end{aligned} \tag{15}$$

$$\begin{aligned}
\mathbf{f}_{m_2} = \hat{\mathbf{M}}_{\mathbf{x},m_2} & \begin{pmatrix} m_{imp_m}^{-1}\left(\alpha_{\mathrm{f}}\mathbf{f}_{hum_1} + (1-\alpha_{\mathrm{f}})\mathbf{f}_{hum_2} - \eta_{\mathrm{f}}\mathbf{f}_{env}^{d}\right) \\ -m_{imp_m}^{-1} b_{imp_m}\dot{\mathbf{x}}_{m_2} - \lambda_{2,m_2}\tilde{\mathbf{x}}_{m_2} - \lambda_{3,m_2}\mathbf{s}_{m_2} \end{pmatrix} \\
& + \hat{\mathbf{C}}_{\mathbf{x},m_2}\dot{\mathbf{x}}_{\mathbf{r},m_2} + \hat{\mathbf{G}}_{\mathbf{x},m_2} + \hat{\mathbf{F}}_{\mathbf{x},m_2} - \mathbf{f}_{hum_2}
\end{aligned} \tag{16}$$

$$\begin{aligned}
\mathbf{f}_s = \hat{\mathbf{M}}_{\mathbf{x},s} & \begin{pmatrix} m_{imp_s}^{-1}(-\mathbf{f}_{env}) + \eta_{\mathrm{x}}(\alpha_{\mathrm{x}}\hat{\dot{\mathbf{x}}}_{m_1}^{d} + (1-\alpha_{\mathrm{x}})\hat{\dot{\mathbf{x}}}_{m_2}^{d}) \\ -m_{imp_s}^{-1} b_{imp_s}(\dot{\mathbf{x}}_s - \eta_{\mathrm{x}}(\alpha_{\mathrm{x}}\dot{\mathbf{x}}_{m_1}^{d} + (1-\alpha_{\mathrm{x}})\dot{\mathbf{x}}_{m_2}^{d})) \\ -m_{imp_s}^{-1} k_{imp_s}(\mathbf{x}_s - \eta_{\mathrm{x}}(\alpha_{\mathrm{x}}\mathbf{x}_{m_1}^{d} + (1-\alpha_{\mathrm{x}})\mathbf{x}_{m_2}^{d})) - \lambda_{3,s}\mathbf{s}_s \end{pmatrix} \\
& + \hat{\mathbf{C}}_{\mathbf{x},s}\dot{\mathbf{x}}_{\mathbf{r},s} + \hat{\mathbf{G}}_{\mathbf{x},s} + \hat{\mathbf{F}}_{\mathbf{x},s} + \mathbf{f}_{env} - \lambda_{4,s}\,\mathrm{sgn}(\mathbf{s}_s)
\end{aligned} \tag{17}$$

where the accent $\wedge$ is used for the estimated matrices, vectors and scalars. λ_{3,m_1} , λ_{3,m_2} , $\lambda_{3,s}$ and $\lambda_{4,s}$ are positive constant parameters. As seen in Eq. (17), the estimation of

masters' accelerations is used in the slave control law. Since the acceleration signals of the masters ($\ddot{\mathbf{x}}_{m_1}^d$ and $\ddot{\mathbf{x}}_{m_2}^d$) are prone to measurement noises, they can be estimated ($\hat{\ddot{\mathbf{x}}}_{m_1}^d$ and $\hat{\ddot{\mathbf{x}}}_{m_2}^d$) in this architecture as the master robots 1 and 2 mimic their reference impedance model (7). For this purpose, the delayed master robots' accelerations ($\ddot{\mathbf{x}}_{m_1}^d$ and $\ddot{\mathbf{x}}_{m_2}^d$) are estimated using Eq. (7) by considering T_1 time delay for all signals as

$$\hat{\ddot{\mathbf{x}}}_{m_l}^d = m_{imp_m}^{-1}\left(\alpha_{\mathrm{f}}\mathbf{f}_{hum_1}^d + (1-\alpha_{\mathrm{f}})\mathbf{f}_{hum_2}^d - \eta_{\mathrm{f}}\,\mathbf{f}_{env}^{dd}\right) - m_{imp_m}^{-1}\,b_{imp_m}\,\dot{\mathbf{x}}_{imp_m}^d \tag{18}$$

for $l=1$ (master 1) and $l=2$ (master 2), where $\mathbf{f}_{env}^{dd}(t)=\mathbf{f}_{env}^{d}(t-T_1)=\mathbf{f}_{env}(t-T_1-T_2)$ has T_1+T_2 time delay, and other signals in (18) with one superscript "d" have T_1 time delay. Moreover, it will be shown that the term $-\lambda_{4,s}\,\mathrm{sgn}(\mathbf{s}_s)$ in Eq. (17) provides robustness of the trilateral control strategy against the bounded estimation error of the master robots' acceleration ($\hat{\ddot{\mathbf{x}}}_{m_1}-\ddot{\mathbf{x}}_{m_1}$ and $\hat{\ddot{\mathbf{x}}}_{m_2}-\ddot{\mathbf{x}}_{m_2}$).

The trilateral control laws (15)-(17) can be represented in a linearly parameterized form based on (4) as

$$\mathbf{f}_{m_1} = \mathbf{R}_{\mathbf{x},m_1}(\xi_{\mathbf{1},m_1},\xi_{\mathbf{2},m_1},\mathbf{q}_{m_1},\dot{\mathbf{q}}_{m_1})\hat{\boldsymbol{\delta}}_{\mathbf{x},m_1} - \mathbf{f}_{hum_1} \tag{19}$$

$$\mathbf{f}_{m_2} = \mathbf{R}_{\mathbf{x},m_2}(\xi_{\mathbf{1},m_2},\xi_{\mathbf{2},m_2},\mathbf{q}_{m_2},\dot{\mathbf{q}}_{m_2})\hat{\boldsymbol{\delta}}_{\mathbf{x},m_2} - \mathbf{f}_{hum_2} \tag{20}$$

$$\mathbf{f}_{s} = \mathbf{R}_{\mathbf{x},s}(\xi_{\mathbf{1},s},\xi_{\mathbf{2},s},\mathbf{q}_{s},\dot{\mathbf{q}}_{s})\hat{\boldsymbol{\delta}}_{\mathbf{x},s} + \mathbf{f}_{env} - \lambda_{4,s}\,\mathrm{sgn}(\mathbf{s}_s) \tag{21}$$

where $\mathbf{R}_{\mathbf{x},m_1}$, $\mathbf{R}_{\mathbf{x},m_2}$ and $\mathbf{R}_{\mathbf{x},s}$ are defined in terms of the following $\xi_{\mathbf{1},m_1}$, $\xi_{\mathbf{1},m_2}$, $\xi_{\mathbf{1},s}$, $\xi_{\mathbf{2},m_1}$, $\xi_{\mathbf{2},m_2}$ and $\xi_{\mathbf{2},s}$ vectors according to (4):

$$\boldsymbol{\xi}_{\mathbf{1},m_1}=\begin{pmatrix} m_{imp_m}^{-1}\left(\alpha_{\mathrm{f}}\mathbf{f}_{hum_1}+(1-\alpha_{\mathrm{f}})\mathbf{f}_{hum_2}-\eta_{\mathrm{f}}\mathbf{f}_{env}^{d}\right) \\ -m_{imp_m}^{-1}b_{imp_m}\dot{\mathbf{x}}_{m_1}-\lambda_{2,m_1}\tilde{\mathbf{x}}_{m_1}-\lambda_{3,m_1}\mathbf{s}_{m_1}\end{pmatrix},\quad \boldsymbol{\xi}_{\mathbf{2},m_1}=\dot{\mathbf{x}}_{\mathbf{r},m_1},$$

$$\boldsymbol{\xi}_{\mathbf{1},m_2}=\begin{pmatrix} m_{imp_m}^{-1}\left(\alpha_{\mathrm{f}}\mathbf{f}_{hum_1}+(1-\alpha_{\mathrm{f}})\mathbf{f}_{hum_2}-\eta_{\mathrm{f}}\mathbf{f}_{env}^{d}\right) \\ -m_{imp_m}^{-1}b_{imp_m}\dot{\mathbf{x}}_{m_2}-\lambda_{2,m_2}\tilde{\mathbf{x}}_{m_2}-\lambda_{3,m_2}\mathbf{s}_{m_2}\end{pmatrix},\quad \boldsymbol{\xi}_{\mathbf{2},m_2}=\dot{\mathbf{x}}_{\mathbf{r},m_2}, \tag{22}$$

$$\boldsymbol{\xi}_{\mathbf{1},s}=\begin{pmatrix} m_{imp_s}^{-1}(-\mathbf{f}_{env})+\eta_{\mathrm{x}}(\alpha_{\mathrm{x}}\hat{\dot{\mathbf{x}}}_{m_1}^{d}+(1-\alpha_{\mathrm{x}})\hat{\dot{\mathbf{x}}}_{m_2}^{d}) \\ -m_{imp_s}^{-1}b_{imp_s}(\dot{\mathbf{x}}_s-\eta_{\mathrm{x}}(\alpha_{\mathrm{x}}\dot{\mathbf{x}}_{m_1}^{d}+(1-\alpha_{\mathrm{x}})\dot{\mathbf{x}}_{m_2}^{d})) \\ -m_{imp_s}^{-1}k_{imp_s}(\mathbf{x}_s-\eta_{\mathrm{x}}(\alpha_{\mathrm{x}}\mathbf{x}_{m_1}^{d}+(1-\alpha_{\mathrm{x}})\mathbf{x}_{m_2}^{d}))-\lambda_{3,s}\mathbf{s}_s\end{pmatrix},\quad \boldsymbol{\xi}_{\mathbf{2},s}=\dot{\mathbf{x}}_{\mathbf{r},s}$$

4.2. Nonlinear Closed-loop System

In this section, the closed-loop dynamics of the dual-user trilateral haptic system is obtained by employing the proposed nonlinear TMRAIC scheme (presented in Sec. 4.1). The control laws (15)-(17) are substituted in the nonlinear dynamics of trilateral haptic system (1)-(3), which yields,

$$\begin{aligned}&\mathbf{M}_{\mathbf{x},m_1}\begin{pmatrix}\ddot{\mathbf{x}}_{m_1}+m_{imp_m}^{-1}b_{imp_m}\dot{\mathbf{x}}_{m_1}+\lambda_{2,m_1}\tilde{\mathbf{x}}_{m_1}\\ -m_{imp_m}^{-1}\left(\alpha_{\mathrm{f}}\mathbf{f}_{hum_1}+(1-\alpha_{\mathrm{f}})\mathbf{f}_{hum_2}-\eta_{\mathrm{f}}\mathbf{f}_{env}^{d}\right)\end{pmatrix}=\\ &\left(\hat{\mathbf{M}}_{\mathbf{x},m_1}-\mathbf{M}_{\mathbf{x},m_1}\right)\begin{pmatrix} m_{imp_m}^{-1}\left(\alpha_{\mathrm{f}}\mathbf{f}_{hum_1}+(1-\alpha_{\mathrm{f}})\mathbf{f}_{hum_2}-\eta_{\mathrm{f}}\mathbf{f}_{env}^{d}\right)\\ -m_{imp_m}^{-1}b_{imp_m}\dot{\mathbf{x}}_{m_1}-\lambda_{2,m_1}\tilde{\mathbf{x}}_{m_1}-\lambda_{3,m_1}\mathbf{s}_{m_1}\end{pmatrix}\\ &+\left(\hat{\mathbf{C}}_{\mathbf{x},m_1}-\mathbf{C}_{\mathbf{x},m_1}\right)\dot{\mathbf{x}}_{\mathbf{r},m_1}+\left(\hat{\mathbf{G}}_{\mathbf{x},m_1}-\mathbf{G}_{\mathbf{x},m_1}\right)+\left(\hat{\mathbf{F}}_{\mathbf{x},m_1}-\mathbf{F}_{\mathbf{x},m_1}\right)-\mathbf{C}_{\mathbf{x},m_1}\mathbf{s}_{m_1}-\lambda_{3,m_1}\mathbf{M}_{\mathbf{x},m_1}\mathbf{s}_{m_1}\end{aligned} \tag{23}$$

$$\begin{aligned}&\mathbf{M}_{\mathbf{x},m_2}\begin{pmatrix}\ddot{\mathbf{x}}_{m_2}+m_{imp_m}^{-1}b_{imp_m}\dot{\mathbf{x}}_{m_2}+\lambda_{2,m_1}\tilde{\mathbf{x}}_{m_2}\\ -m_{imp_m}^{-1}\left(\alpha_{\mathrm{f}}\mathbf{f}_{hum_1}+(1-\alpha_{\mathrm{f}})\mathbf{f}_{hum_2}-\eta_{\mathrm{f}}\mathbf{f}_{env}^{d}\right)\end{pmatrix}=\\ &\left(\hat{\mathbf{M}}_{\mathbf{x},m_2}-\mathbf{M}_{\mathbf{x},m_2}\right)\begin{pmatrix} m_{imp_m}^{-1}\left(\alpha_{\mathrm{f}}\mathbf{f}_{hum_1}+(1-\alpha_{\mathrm{f}})\mathbf{f}_{hum_2}-\eta_{\mathrm{f}}\mathbf{f}_{env}^{d}\right)\\ -m_{imp_m}^{-1}b_{imp_m}\dot{\mathbf{x}}_{m_2}-\lambda_{2,m_2}\tilde{\mathbf{x}}_{m_2}-\lambda_{3,m_2}\mathbf{s}_{m_2}\end{pmatrix}\\ &+\left(\hat{\mathbf{C}}_{\mathbf{x},m_2}-\mathbf{C}_{\mathbf{x},m_2}\right)\dot{\mathbf{x}}_{\mathbf{r},m_2}+\left(\hat{\mathbf{G}}_{\mathbf{x},m_2}-\mathbf{G}_{\mathbf{x},m_2}\right)+\left(\hat{\mathbf{F}}_{\mathbf{x},m_2}-\mathbf{F}_{\mathbf{x},m_2}\right)-\mathbf{C}_{\mathbf{x},m_2}\mathbf{s}_{m_2}-\lambda_{3,m_2}\mathbf{M}_{\mathbf{x},m_2}\mathbf{s}_{m_2}\end{aligned} \tag{24}$$

$$\mathbf{M}_{\mathbf{x},s}\begin{pmatrix}(\ddot{\mathbf{x}}_s-\eta_{\mathrm{x}}(\alpha_{\mathrm{x}}\ddot{\mathbf{x}}^d_{m_1}+(1-\alpha_{\mathrm{x}})\ddot{\mathbf{x}}^d_{m_2}))\\+m^{-1}_{imp_s}b_{imp_s}(\dot{\mathbf{x}}_s-\eta_{\mathrm{x}}(\alpha_{\mathrm{x}}\dot{\mathbf{x}}^d_{m_1}+(1-\alpha_{\mathrm{x}})\dot{\mathbf{x}}^d_{m_2}))\\+m^{-1}_{imp_s}k_{imp_s}(\mathbf{x}_s-\eta_{\mathrm{x}}(\alpha_{\mathrm{x}}\mathbf{x}^d_{m_1}+(1-\alpha_{\mathrm{x}})\mathbf{x}^d_{m_2}))\\-m^{-1}_{imp_s}(-\mathbf{f}_{env})\end{pmatrix}=$$

$$\mathbf{M}_{\mathbf{x},s}\eta_{\mathrm{x}}\left(\alpha_{\mathrm{x}}(\hat{\ddot{\mathbf{x}}}^d_{m_1}-\ddot{\mathbf{x}}^d_{m_1})+(1-\alpha_{\mathrm{x}})(\hat{\ddot{\mathbf{x}}}^d_{m_2}-\ddot{\mathbf{x}}^d_{m_2})\right) \tag{25}$$

$$+\left(\hat{\mathbf{M}}_{\mathbf{x},s}-\mathbf{M}_{\mathbf{x},s}\right)\begin{pmatrix}m^{-1}_{imp_s}(-\mathbf{f}_{env})+\eta_{\mathrm{x}}(\alpha_{\mathrm{x}}\hat{\ddot{\mathbf{x}}}^d_{m_1}+(1-\alpha_{\mathrm{x}})\hat{\ddot{\mathbf{x}}}^d_{m_2})\\-m^{-1}_{imp_s}b_{imp_s}(\dot{\mathbf{x}}_s-\eta_{\mathrm{x}}(\alpha_{\mathrm{x}}\dot{\mathbf{x}}^d_{m_1}+(1-\alpha_{\mathrm{x}})\dot{\mathbf{x}}^d_{m_2}))\\-m^{-1}_{imp_s}k_{imp_s}(\mathbf{x}_s-\eta_{\mathrm{x}}(\alpha_{\mathrm{x}}\mathbf{x}^d_{m_1}+(1-\alpha_{\mathrm{x}})\mathbf{x}^d_{m_2}))-\lambda_{3,s}\mathbf{s}_s\end{pmatrix}$$

$$+\left(\hat{\mathbf{C}}_{\mathbf{x},s}-\mathbf{C}_{\mathbf{x},s}\right)\dot{\mathbf{x}}_{\mathbf{r},s}+\left(\hat{\mathbf{G}}_{\mathbf{x},s}-\mathbf{G}_{\mathbf{x},s}\right)+\left(\hat{\mathbf{F}}_{\mathbf{x},s}-\mathbf{F}_{\mathbf{x},s}\right)-\mathbf{C}_{\mathbf{x},s}\mathbf{s}_s-\lambda_{3,s}\mathbf{M}_{\mathbf{x},s}\mathbf{s}_s-\lambda_{4,s}\,\mathrm{sgn}(\mathbf{s}_s)$$

Now, the master reference impedance model (7) is multiplied by $\mathbf{M}_{\mathbf{x},m_1}m^{-1}_{imp_m}$ and subtracted from (23) and (24), and the slave reference impedance model (8) is multiplied by $\mathbf{M}_{\mathbf{x},s}m^{-1}_{imp_s}$ and subtracted from (25). Then, using Eq. (4) and based on Eq. (22), Eqs. (23)-(25) are reduced to

$$\mathbf{M}_{\mathbf{x},m_1}\left(\ddot{\tilde{\mathbf{x}}}_{m_1}+m^{-1}_{imp_m}b_{imp_m}\dot{\tilde{\mathbf{x}}}_{m_1}+\lambda_{2,m_1}\tilde{\mathbf{x}}_{m_1}\right)=\mathbf{R}_{\mathbf{x},m_1}\tilde{\boldsymbol{\delta}}_{\mathbf{x},m_1}-\mathbf{C}_{\mathbf{x},m_1}\mathbf{s}_{m_1}-\lambda_{3,m_1}\mathbf{M}_{\mathbf{x},m_1}\mathbf{s}_{m_1} \tag{26}$$

$$\mathbf{M}_{\mathbf{x},m_2}\left(\ddot{\tilde{\mathbf{x}}}_{m_2}+m^{-1}_{imp_m}b_{imp_m}\dot{\tilde{\mathbf{x}}}_{m_2}+\lambda_{2,m_1}\tilde{\mathbf{x}}_{m_2}\right)=\mathbf{R}_{\mathbf{x},m_2}\tilde{\boldsymbol{\delta}}_{\mathbf{x},m_2}-\mathbf{C}_{\mathbf{x},m_2}\mathbf{s}_{m_2}-\lambda_{3,m_2}\mathbf{M}_{\mathbf{x},m_2}\mathbf{s}_{m_2} \tag{27}$$

$$\begin{aligned}\mathbf{M}_{\mathbf{x},s}\left(\ddot{\tilde{\mathbf{x}}}_s+m^{-1}_{imp_s}b_{imp_s}\dot{\tilde{\mathbf{x}}}_s+m^{-1}_{imp_s}k_{imp_s}\tilde{\mathbf{x}}_s\right)&=\mathbf{R}_{\mathbf{x},s}\tilde{\boldsymbol{\delta}}_{\mathbf{x},s}-\mathbf{C}_{\mathbf{x},s}\mathbf{s}_s-\lambda_{3,s}\mathbf{M}_{\mathbf{x},s}\mathbf{s}_s\\&+\mathbf{M}_{\mathbf{x},s}\eta_{\mathrm{x}}\left(\alpha_{\mathrm{x}}(\hat{\ddot{\mathbf{x}}}^d_{m_1}-\ddot{\mathbf{x}}^d_{m_1})+(1-\alpha_{\mathrm{x}})(\hat{\ddot{\mathbf{x}}}^d_{m_2}-\ddot{\mathbf{x}}^d_{m_2})\right)-\lambda_{4,s}\,\mathrm{sgn}(\mathbf{s}_s)\end{aligned} \tag{28}$$

where $\tilde{\boldsymbol{\delta}}_{\mathbf{x},m_1}=\hat{\boldsymbol{\delta}}_{\mathbf{x},m_1}-\boldsymbol{\delta}_{\mathbf{x},m_1}$, $\tilde{\boldsymbol{\delta}}_{\mathbf{x},m_2}=\hat{\boldsymbol{\delta}}_{\mathbf{x},m_2}-\boldsymbol{\delta}_{\mathbf{x},m_2}$ and $\tilde{\boldsymbol{\delta}}_{\mathbf{x},s}=\hat{\boldsymbol{\delta}}_{\mathbf{x},s}-\boldsymbol{\delta}_{\mathbf{x},s}$ are the estimation error vectors for the master 1, master 2 and the slave robots, respectively. Finally, by substituting the time derivatives of the sliding surfaces (13) in the left side of Eqs. (26)-(28), the closed-loop dynamics of the trilateral haptic system is obtained as

$$\mathbf{M}_{\mathbf{x},m_1}\dot{\mathbf{s}}_{m_1}=\mathbf{R}_{\mathbf{x},m_1}\tilde{\boldsymbol{\delta}}_{\mathbf{x},m_1}-\mathbf{C}_{\mathbf{x},m_1}\mathbf{s}_{m_1}-\lambda_{3,m_1}\mathbf{M}_{\mathbf{x},m_1}\mathbf{s}_{m_1} \tag{29}$$

$$\mathbf{M}_{\mathbf{x},m_2}\dot{\mathbf{s}}_{m_2}=\mathbf{R}_{\mathbf{x},m_2}\tilde{\boldsymbol{\delta}}_{\mathbf{x},m_2}-\mathbf{C}_{\mathbf{x},m_2}\mathbf{s}_{m_2}-\lambda_{3,m_2}\mathbf{M}_{\mathbf{x},m_2}\mathbf{s}_{m_2} \tag{30}$$

$$\begin{aligned}\mathbf{M}_{\mathbf{x},s}\dot{\mathbf{s}}_s=&\mathbf{R}_{\mathbf{x},s}\tilde{\boldsymbol{\delta}}_{\mathbf{x},s}-\mathbf{C}_{\mathbf{x},s}\mathbf{s}_s-\lambda_{3,s}\mathbf{M}_{\mathbf{x},s}\mathbf{s}_s-\lambda_{4,s}\,\mathrm{sgn}(\mathbf{s}_s)\\&+\mathbf{M}_{\mathbf{x},s}\eta_{\mathrm{x}}\left(\alpha_{\mathrm{x}}(\hat{\ddot{\mathbf{x}}}^d_{m_1}-\ddot{\mathbf{x}}^d_{m_1})+(1-\alpha_{\mathrm{x}})(\hat{\ddot{\mathbf{x}}}^d_{m_2}-\ddot{\mathbf{x}}^d_{m_2})\right)\end{aligned} \tag{31}$$

According to above-mentioned trilateral MRAIC scheme, the master and slave impedance parameters ($m^{-1}_{imp_m}b_{imp_m}$, $m^{-1}_{imp_s}b_{imp_s}$ and $m^{-1}_{imp_s}k_{imp_s}$) are employed in the control laws (15)-(17) and the sliding surfaces (13).

4.3. Lyapunov-based Proof of Tracking Convergence and Required Adaptation Laws

In this section, the tracking convergences of the master robots' trajectories to the response of master reference model ($\mathbf{x}_{m_1}\to\mathbf{x}_{imp_m}$, $\mathbf{x}_{m_2}\to\mathbf{x}_{imp_m}$) and the slave robot's trajectory to the response of slave reference model ($\mathbf{x}_s\to\mathbf{x}_{imp_s}$) are proven. To this end, a positive definite Lyapunov function candidate is suggested as

$$V(t)=\frac{1}{2}\left(\begin{aligned}&\mathbf{s}^T_{m_1}\mathbf{M}_{\mathbf{x},m_1}\mathbf{s}_{m_1}+\mathbf{s}^T_{m_2}\mathbf{M}_{\mathbf{x},m_2}\mathbf{s}_{m_2}+\mathbf{s}^T_s\mathbf{M}_{\mathbf{x},s}\mathbf{s}_s\\&+\tilde{\boldsymbol{\delta}}^T_{\mathbf{x},m_1}\mathbf{H}^{-1}_{m_1}\tilde{\boldsymbol{\delta}}_{\mathbf{x},m_1}+\tilde{\boldsymbol{\delta}}^T_{\mathbf{x},m_2}\mathbf{H}^{-1}_{m_2}\tilde{\boldsymbol{\delta}}_{\mathbf{x},m_2}+\tilde{\boldsymbol{\delta}}^T_{\mathbf{x},s}\mathbf{H}^{-1}_{s}\tilde{\boldsymbol{\delta}}_{\mathbf{x},s}\end{aligned}\right) \tag{32}$$

where $\mathbf{H}_{m_1}$, $\mathbf{H}_{m_2}$ and $\mathbf{H}_s$ are constant symmetric positive definite matrices that will act as the gains of adaptation laws. The time derivative of V is then determined:

$$\begin{aligned}\dot{V}(t)=&\mathbf{s}^T_{m_1}\left(\mathbf{M}_{\mathbf{x},m_1}\dot{\mathbf{s}}_{m_1}+\frac{1}{2}\dot{\mathbf{M}}_{\mathbf{x},m_1}\mathbf{s}_{m_1}\right)+\dot{\hat{\tilde{\boldsymbol{\delta}}}}^T_{\mathbf{x},m_1}\mathbf{H}^{-1}_{m_1}\tilde{\boldsymbol{\delta}}_{\mathbf{x},m_1}\\&+\mathbf{s}^T_{m_2}\left(\mathbf{M}_{\mathbf{x},m_2}\dot{\mathbf{s}}_{m_2}+\frac{1}{2}\dot{\mathbf{M}}_{\mathbf{x},m_2}\mathbf{s}_{m_2}\right)+\dot{\hat{\tilde{\boldsymbol{\delta}}}}^T_{\mathbf{x},m_2}\mathbf{H}^{-1}_{m_2}\tilde{\boldsymbol{\delta}}_{\mathbf{x},m_2}\\&+\mathbf{s}^T_{s}\left(\mathbf{M}_{\mathbf{x},s}\dot{\mathbf{s}}_{s}+\frac{1}{2}\dot{\mathbf{M}}_{\mathbf{x},s}\mathbf{s}_{s}\right)+\dot{\hat{\tilde{\boldsymbol{\delta}}}}^T_{\mathbf{x},s}\mathbf{H}^{-1}_{s}\tilde{\boldsymbol{\delta}}_{\mathbf{x},s}\end{aligned} \tag{33}$$

where $\dot{\tilde{\boldsymbol{\delta}}}_{\mathbf{x},j} = \dot{\hat{\boldsymbol{\delta}}}_{\mathbf{x},j}$ (for $j = m_1, m_2, s$) because $\tilde{\boldsymbol{\delta}}_{\mathbf{x},j} = \hat{\boldsymbol{\delta}}_{\mathbf{x},j} - \boldsymbol{\delta}_{\mathbf{x},j}$ and $\boldsymbol{\delta}_{\mathbf{x},j}$ is the vector of unknown real parameters that is constant: $\dot{\boldsymbol{\delta}}_{\mathbf{x},j} = 0$. Substituting the final dynamics of closed-loop trilateral haptic system (29)-(31) in Eq. (33) yields to:

$$\begin{aligned}\dot{V}(t) = {} & \mathbf{s}_{m_1}^T \mathbf{R}_{\mathbf{x},m_1} \tilde{\boldsymbol{\delta}}_{\mathbf{x},m_1} + \dot{\hat{\boldsymbol{\delta}}}_{\mathbf{x},m_1}^T \mathbf{H}_{m_1}^{-1} \tilde{\boldsymbol{\delta}}_{\mathbf{x},m_1} + \frac{1}{2}\mathbf{s}_{m_1}^T \left(\dot{\mathbf{M}}_{\mathbf{x},m_1} - 2\mathbf{C}_{\mathbf{x},m_1}\right)\mathbf{s}_{m_1} - \lambda_{3,m_1}\mathbf{s}_{m_1}^T \mathbf{M}_{\mathbf{x},m_1}\mathbf{s}_{m_1} \\ & + \mathbf{s}_{m_2}^T \mathbf{R}_{\mathbf{x},m_2} \tilde{\boldsymbol{\delta}}_{\mathbf{x},m_2} + \dot{\hat{\boldsymbol{\delta}}}_{\mathbf{x},m_2}^T \mathbf{H}_{m_2}^{-1} \tilde{\boldsymbol{\delta}}_{\mathbf{x},m_2} + \frac{1}{2}\mathbf{s}_{m_2}^T \left(\dot{\mathbf{M}}_{\mathbf{x},m_2} - 2\mathbf{C}_{\mathbf{x},m_2}\right)\mathbf{s}_{m_2} - \lambda_{3,m_2}\mathbf{s}_{m_2}^T \mathbf{M}_{\mathbf{x},m_2}\mathbf{s}_{m_2} \\ & + \mathbf{s}_s^T \mathbf{R}_{\mathbf{x},s} \tilde{\boldsymbol{\delta}}_{\mathbf{x},s} + \dot{\hat{\boldsymbol{\delta}}}_{\mathbf{x},s}^T \mathbf{H}_s^{-1} \tilde{\boldsymbol{\delta}}_{\mathbf{x},s} + \frac{1}{2}\mathbf{s}_s^T \left(\dot{\mathbf{M}}_{\mathbf{x},s} - 2\mathbf{C}_{\mathbf{x},s}\right)\mathbf{s}_s - \lambda_{3,s}\mathbf{s}_s^T \mathbf{M}_{\mathbf{x},s}\mathbf{s}_s \\ & + \mathbf{s}_s^T \left(\mathbf{M}_{\mathbf{x},s}\eta_{\mathrm{x}} \left(\alpha_{\mathrm{x}}(\hat{\ddot{\mathbf{x}}}_{m_1}^d - \ddot{\mathbf{x}}_{m_1}^d) + (1-\alpha_{\mathrm{x}})(\hat{\ddot{\mathbf{x}}}_{m_2}^d - \ddot{\mathbf{x}}_{m_2}^d)\right) - \lambda_{4,s}\,\mathrm{sgn}(\mathbf{s}_s)\right)\end{aligned} \tag{34}$$

Now, three adaptation laws for updating the estimated dynamic parameters of the master 1, master 2 and slave are defined as

$$\dot{\hat{\boldsymbol{\delta}}}_{\mathbf{x},m_1} = -\mathbf{H}_{m_1}^T \mathbf{R}_{\mathbf{x},m_1}\mathbf{s}_{m_1},\ \ \dot{\hat{\boldsymbol{\delta}}}_{\mathbf{x},m_2} = -\mathbf{H}_{m_2}^T \mathbf{R}_{\mathbf{x},m_2}\mathbf{s}_{m_2},\ \ \dot{\hat{\boldsymbol{\delta}}}_{\mathbf{x},s} = -\mathbf{H}_s^T \mathbf{R}_{\mathbf{x},s}\mathbf{s}_s \tag{35}$$

By substituting the adaptation laws (35) in the time derivative of the Lyapunov function (34) and employing the robots' property that $\dot{\mathbf{M}}_{\mathbf{x},j} - 2\mathbf{C}_{\mathbf{x},j}$ is skew symmetric, $\dot{V}$ is obtained as

$$\begin{aligned}\dot{V}(t) = {} & -\lambda_{3,m_1}\mathbf{s}_{m_1}^T \mathbf{M}_{\mathbf{x},m_1}\mathbf{s}_{m_1} - \lambda_{3,m_2}\mathbf{s}_{m_2}^T \mathbf{M}_{\mathbf{x},m_2}\mathbf{s}_{m_2} - \lambda_{3,s}\mathbf{s}_s^T \mathbf{M}_{\mathbf{x},s}\mathbf{s}_s \\ & + \mathbf{s}_s^T \left(\mathbf{M}_{\mathbf{x},s}\eta_{\mathrm{x}} \left(\alpha_{\mathrm{x}}(\hat{\ddot{\mathbf{x}}}_{m_1}^d - \ddot{\mathbf{x}}_{m_1}^d) + (1-\alpha_{\mathrm{x}})(\hat{\ddot{\mathbf{x}}}_{m_2}^d - \ddot{\mathbf{x}}_{m_2}^d)\right) - \lambda_{4,s}\,\mathrm{sgn}(\mathbf{s}_s)\right)\end{aligned} \tag{36}$$

To provide robustness against the bounded estimation errors of the masters' accelerations ($\hat{\ddot{\mathbf{x}}}_{m_1} - \ddot{\mathbf{x}}_{m_1}$ and $\hat{\ddot{\mathbf{x}}}_{m_2} - \ddot{\mathbf{x}}_{m_2}$), the positive constant parameter $\lambda_{4,s}$ in the slave control law (17) should be chosen such that the following inequality is satisfied:

$$\lambda_{4,s} \geq \left\| \mathbf{M}_{\mathbf{x},s}\eta_{\mathrm{x}} \left(\alpha_{\mathrm{x}}(\hat{\ddot{\mathbf{x}}}_{m_1}^d - \ddot{\mathbf{x}}_{m_1}^d) + (1-\alpha_{\mathrm{x}})(\hat{\ddot{\mathbf{x}}}_{m_2}^d - \ddot{\mathbf{x}}_{m_2}^d)\right) \right\|_\infty \tag{37}$$

Note that the errors of acceleration estimation ($\hat{\ddot{\mathbf{x}}}_{m_1} - \ddot{\mathbf{x}}_{m_1}$, $\hat{\ddot{\mathbf{x}}}_{m_2} - \ddot{\mathbf{x}}_{m_2}$) are unknown, and the parameters in $\mathbf{M}_{\mathbf{x},s}$ have uncertainty in this trilateral adaptive controller. However, based on (37), the maximum value of $\left\| \mathbf{M}_{\mathbf{x},s} \eta_{\mathrm{x}} \left(\alpha_{\mathrm{x}} (\hat{\ddot{\mathbf{x}}}^d_{m_1} - \ddot{\mathbf{x}}^d_{m_1}) + (1-\alpha_{\mathrm{x}})(\hat{\ddot{\mathbf{x}}}^d_{m_2} - \ddot{\mathbf{x}}^d_{m_2}) \right) \right\|_\infty$ should be bounded and $\lambda_{4,s}$ should be chosen larger than its upper bound to have the stability. Then, the time derivative of the Lyapunov function (36) can be written as

$$\dot{V}(t) \le -\lambda_{3,m_1} \mathbf{s}_{m_1}^T \mathbf{M}_{\mathbf{x},m_1} \mathbf{s}_{m_1} - \lambda_{3,m_2} \mathbf{s}_{m_2}^T \mathbf{M}_{\mathbf{x},m_2} \mathbf{s}_{m_2} - \lambda_{3,s} \mathbf{s}_s^T \mathbf{M}_{\mathbf{x},s} \mathbf{s}_s \tag{38}$$

***Theorem*.** Due to the uniform positive definiteness of inertia matrices ($\mathbf{M}_{\mathbf{x},m_1}$, $\mathbf{M}_{\mathbf{x},m_2}$ and $\mathbf{M}_{\mathbf{x},s}$) and adaptation gains ($\mathbf{H}_{m_1}$, $\mathbf{H}_{m_2}$ and $\mathbf{H}_s$), the Lyapunov function (32) is positive definite ($V(t) > 0$) and its time derivative (38) is negative semi-definite ($\dot{V}(t) \le 0$). Thus, the convergence to sliding surfaces ($\mathbf{s}_{m_1} = 0$, $\mathbf{s}_{m_2} = 0$ and $\mathbf{s}_s = 0$) and the boundedness of parameter estimation errors ($\tilde{\boldsymbol{\delta}}_{\mathbf{x},m_1}$, $\tilde{\boldsymbol{\delta}}_{\mathbf{x},m_2}$ and $\tilde{\boldsymbol{\delta}}_{\mathbf{x},s}$) are ensured.

***Proof*.** Regarding Eq. (38) and considering $g(t) = \lambda_{3,m_1} \mathbf{s}_{m_1}^T \mathbf{M}_{\mathbf{x},m_1} \mathbf{s}_{m_1} + \lambda_{3,m_2} \mathbf{s}_{m_2}^T \mathbf{M}_{\mathbf{x},m_2} \mathbf{s}_{m_2} + \lambda_{3,s} \mathbf{s}_s^T \mathbf{M}_{\mathbf{x},s} \mathbf{s}_s \ge 0$ as a uniform continuous function, one can write

$$V(0) - V(\infty) \ge \lim_{t \to \infty} \int_0^t g(\phi)\, d\phi \tag{39}$$

Moreover, $\dot{V}(t) = dV(t)/dt \le 0$ is negative semi-definite based on Eq. (38), which implies that $V(0) - V(\infty) \ge 0$ is positive and finite. Therefore, $\lim_{t \to \infty} \int_0^t g(\phi)\, d\phi$ in (39) exists and has a finite and positive value based on the positiveness of $g(t)$. Consequently, according to the Barbalat lemma [43]:

$$\lim_{t\to\infty} g(t) = \lim_{t\to\infty}\left(\lambda_{3,m_1}\mathbf{s}_{m_1}^T\mathbf{M}_{\mathbf{x},m_1}\mathbf{s}_{m_1} + \lambda_{3,m_2}\mathbf{s}_{m_2}^T\mathbf{M}_{\mathbf{x},m_2}\mathbf{s}_{m_2} + \lambda_{3,s}\mathbf{s}_s^T\mathbf{M}_{\mathbf{x},s}\mathbf{s}_s\right) = 0 \quad (40)$$

Since $\lambda_{3,m_1} > 0$, $\lambda_{3,m_1} > 0$ and $\lambda_{3,s} > 0$ are non-zero constants, $\mathbf{s}_{m_1}^T\mathbf{M}_{\mathbf{x},m_1}\mathbf{s}_{m_1} \geq 0$, $\mathbf{s}_{m_1}^T\mathbf{M}_{\mathbf{x},m_1}\mathbf{s}_{m_1} \geq 0$ and $\mathbf{s}_s^T\mathbf{M}_{\mathbf{x},s}\mathbf{s}_s \geq 0$, Eq. (40) implies the convergence to sliding surfaces ($\mathbf{s}_{m_1} = 0$, $\mathbf{s}_{m_2} = 0$ and $\mathbf{s}_s = 0$) as $t \to \infty$. Since $V(t) > 0$ and $\dot{V}(t) \leq 0$, the Lyapunov function (32) remains bounded. As a result, the convergence of $\mathbf{s}_{m_1} \to 0$, $\mathbf{s}_{m_2} \to 0$ and $\mathbf{s}_s \to 0$ together with the boundedness of $V(t)$ in Eq. (32) imply that the errors of parameter identification ($\tilde{\boldsymbol{\delta}}_{\mathbf{x},m_1}$, $\tilde{\boldsymbol{\delta}}_{\mathbf{x},m_2}$ and $\tilde{\boldsymbol{\delta}}_{\mathbf{x},s}$) remain bounded. This concludes the proof.

According to the stable dynamics of the masters and slave sliding surfaces defined in (13), the tracking errors also converge to zero ($\tilde{\mathbf{x}}_{m_1} \to 0$, $\tilde{\mathbf{x}}_{m_2} \to 0$ and $\tilde{\mathbf{x}}_s \to 0$) on the surfaces of $\mathbf{s}_{m_1} = 0$, $\mathbf{s}_{m_2} = 0$ and $\mathbf{s}_s = 0$. As a result, the master 1, master 2 and slave track their desired trajectories (i.e., $\mathbf{x}_{m_1} \to \mathbf{x}_{imp_m}$, $\mathbf{x}_{m_2} \to \mathbf{x}_{imp_m}$ and $\mathbf{x}_s \to \mathbf{x}_{imp_s}$), which is the objective of the proposed nonlinear trilateral controller.

5. ABSOLUTE STABILITY OF TRILATERAL HAPTIC SYSTEM SUBJECTED TO TIME DELAYS

After the tracking convergence proof for the masters and slave robots, the absolute stability [39] of the trilateral haptic system is investigated using the proposed TMRAIC scheme in this section. Absolute stability [39, 47, 48] is a well-known tool for the stability analysis of two-port teleoperation systems, which is tested using the Llewellyn's criterion. This criterion guarantees the stability of a coupled system including a two-port network connected to two passive but otherwise arbitrary terminations [39].

Recently, the Llewellyn's absolute stability criterion has been extended to three-port network systems in [40]. Accordingly, it is shown in this section that the proposed TMRAIC method can provide the absolute stability of trilateral haptic systems in the presence of bounded communication delays through the suitable adjustment of impedance parameters.

For this purpose, the relation between the interaction forces ($f_{hum_1,i}$, $f_{hum_2,i}$, $f_{env,i}$) and robots velocities ($\dot{x}_{m_1,i}$, $\dot{x}_{m_2,i}$, $\dot{x}_{s,i}$) of the trilateral system, in each direction (i) of the Cartesian space, is defined in terms of a hybrid matrix $\mathbf{H}_i$ as

$$\begin{bmatrix} F_{hum_1,i}(s) \\ V_{m_2,i}(s) \\ V_{s,i}(s) \end{bmatrix} = \underbrace{\begin{bmatrix} h_{11,i} & h_{12,i} & h_{13,i} \\ h_{21,i} & h_{22,i} & h_{23,i} \\ h_{31,i} & h_{32,i} & h_{33,i} \end{bmatrix}}_{\mathbf{H}_i} \begin{bmatrix} V_{m_1,i}(s) \\ F_{hum_2,i}(s) \\ -F_{env,i}(s) \end{bmatrix} \tag{41}$$

where $F_{hum_1,i}(s)$, $F_{hum_2,i}(s)$, $F_{env,i}(s)$, $V_{m_1,i}(s)$, $V_{m_2,i}(s)$ and $V_{s,i}(s)$ are the Laplace transforms of $f_{hum_1,i}$, $f_{hum_2,i}$, $f_{env,i}$, $\dot{x}_{m_1,i}$, $\dot{x}_{m_2,i}$ and $\dot{x}_{s,i}$, respectively. The sufficient conditions for the absolute stability of trilateral systems in terms of the elements of hybrid matrix $\mathbf{H}_i$ have been introduced in [40, 49] as

(a) The elements of $\mathbf{H}_i$ do not have any pole in the right half of the complex plane (RHP).

(b) Any pole of the elements of $\mathbf{H}_i$ that exists on the imaginary axis should be simple with real and positive residue.

(c) The following symmetrization condition is satisfied:

$$h_{13,i}\, h_{21,i}\, h_{32,i} - h_{12,i}\, h_{23,i}\, h_{31,i} = 0 \tag{42}$$

(d) The following inequalities are satisfied for the real values of ω ($s = j\omega$):

$$\beta_1(\omega) = \mathrm{Re}(h_{11,i}) \geq 0 \tag{43a}$$

$$\beta_2(\omega) = \mathrm{Re}(h_{22,i}) \geq 0 \tag{43b}$$

$$\beta_3(\omega) = \mathrm{Re}(h_{33,i}) \geq 0 \tag{43c}$$

$$\beta_4(\omega) = 2\mathrm{Re}(h_{11,i})\mathrm{Re}(h_{22,i}) - \mathrm{Re}(h_{12,i}h_{21,i}) - \left|h_{12,i}h_{21,i}\right| \geq 0 \tag{44a}$$

$$\beta_5(\omega) = 2\mathrm{Re}(h_{11,i})\mathrm{Re}(h_{33,i}) - \mathrm{Re}(h_{13,i}h_{31,i}) - \left|h_{13,i}h_{31,i}\right| \geq 0 \tag{44b}$$

$$\beta_6(\omega) = 2\mathrm{Re}(h_{22,i})\mathrm{Re}(h_{33,i}) - \mathrm{Re}(h_{23,i}h_{32,i}) - \left|h_{23,i}h_{32,i}\right| \geq 0 \tag{44c}$$

$$\begin{aligned}\beta_7(\omega) = {} & 2\mathrm{Re}(h_{11,i})\mathrm{Re}(h_{22,i})\mathrm{Re}(h_{33,i}) \\ & - \mathrm{Re}(h_{11,i})\left(\mathrm{Re}(h_{23,i}h_{32,i}) + \left|h_{23,i}h_{32,i}\right|\right) \\ & - \mathrm{Re}(h_{22,i})\left(\mathrm{Re}(h_{13,i}h_{31,i}) + \left|h_{13,i}h_{31,i}\right|\right) \\ & - \mathrm{Re}(h_{33,i})\left(\mathrm{Re}(h_{12,i}h_{21,i}) + \left|h_{12,i}h_{21,i}\right|\right) \\ & + 2\mathrm{Re}(\sqrt{h_{12,i}h_{21,i}})\mathrm{Re}(\sqrt{h_{13,i}h_{31,i}})\mathrm{Re}(\sqrt{h_{23,i}h_{32,i}}) \geq 0\end{aligned} \tag{45}$$

Here, β_1 to β_7 are called the absolute stability indices. If the hybrid matrix elements $\mathbf{H}_i$ satisfy the above conditions, the trilateral haptic system is absolutely stable, i.e., the master 1, master 2 and slave will be stable during their physical interactions with any passive human operators and any passive environment.

Based on the position tracking convergence proven in Sec. 4.3, the masters 1 and 2 track the response of master impedance model (7): $\mathbf{x}_{m_1} \to \mathbf{x}_{imp_m}$, $\mathbf{x}_{m_2} \to \mathbf{x}_{imp_m}$, and the slave tracks the response of slave impedance model (8): $\mathbf{x}_s \to \mathbf{x}_{imp_s}$. In addition to the position tracking performance, the closed-loop dynamics of the masters and the slave are made similar to their corresponding reference impedance models (7) and (8),

respectively, by utilizing the suitable impedance parameters in the proposed nonlinear TMRAIC structure (13)-(17). As a result of these conditions, the hybrid matrix of the proposed controlled trilateral haptic system in each direction i of Cartesian space is obtained as

$$\mathbf{H}_i = \begin{bmatrix} \dfrac{m_{imp_m} s + b_{imp_m}}{\alpha_{\mathrm{f}}} & \dfrac{\alpha_{\mathrm{f}} - 1}{\alpha_{\mathrm{f}}} & \dfrac{-\eta_{\mathrm{f}}\, \mathrm{e}^{-T_2 s}}{\alpha_{\mathrm{f}}} \\ 1 & 0 & 0 \\ \eta_{\mathrm{x}}\, \mathrm{e}^{-T_1 s} & 0 & \dfrac{s}{m_{imp_s} s^2 + b_{imp_s} s + k_{imp_s}} \end{bmatrix} \tag{46}$$

The first row of above matrix comes from mimicking the reference impedance model (7) and tracking its response by the master 1 using the corresponding MRAIC law (15). As master 2 tracks the response of master impedance model ($\mathbf{x}_{m_2} \to \mathbf{x}_{imp_m}$) via its controller (16), similar to the master 1 ($\mathbf{x}_{m_1} \to \mathbf{x}_{imp_m}$), one can write $\mathbf{x}_{m_2} \to \mathbf{x}_{m_1}$ which is represented in the second row of hybrid matrix in Eq. (46). The third row of $\mathbf{H}_i$ comes from mimicking the reference impedance model (8) and tracking its response by the slave robot using the corresponding MRAIC law (17). Note that as a result of tracking convergence, the master 2 trajectory converges to the same response as the master 1 ($\mathbf{x}_{m_2} \to \mathbf{x}_{m_1}$); therefore, the total masters trajectory used in the slave impedance model (8) will be: $(\alpha_{\mathrm{x}} \mathbf{x}^d_{m_1} + (1-\alpha_{\mathrm{x}}) \mathbf{x}^d_{m_2}) \to \mathbf{x}^d_{m_1}$, as reflected in the third row of $\mathbf{H}_i$ in Eq. (46).

Accordingly, the symmetrization condition (c) and inequalities (43b), (44a), (44c) and (45) in the condition (d) of the absolute stability are satisfied based on the final hybrid matrix (46). The conditions (a), (b), (43a) and (43c) imply that the positive impedance parameters should be employed. Moreover, the condition (44b) of trilateral

absolute stability enforces an additional inequality for the impedance parameters that is obtained after simplifications as

$$\beta_5(\omega)=\frac{b_{imp_m}b_{imp_s}\omega^2}{b_{imp_s}^2\omega^2+\left(k_{imp_s}-m_{imp_s}\omega^2\right)^2}-\frac{\eta_f\eta_x}{2}\left[1-\cos\left((T_1+T_2)\omega\right)\right]\geq 0 \qquad (47)$$

As a result, if the chosen positive impedance parameters for masters and the slave satisfy inequality (47) for the stability index β_5 in the range of operating frequencies, the proposed trilateral haptic system is absolutely stable. In the absence of time delays in communication channels ($T_1=T_2=0$), arbitrary positive impedance parameters will satisfy Eq. (47). However, in the presence of communication delays ($T_1\neq 0$ and/or $T_2\neq 0$), the impedance parameters b_{imp_m}, k_{imp_s}, b_{imp_s} and m_{imp_s} should be adjusted appropriately in order to satisfy (47) for all working frequencies ω. Then, the absolute stability of three-port teleoperation system in the presence of time delays is guaranteed.

5.1. Adjustment of Impedance parameters for Absolute Stability

The initial master and slave impedance parameters should be chosen in each application based on the desired characteristics of the trilateral haptic system. For example, the appropriate impedance adjustment for the transparency condition (perfect position synchronization and force reflection) was described in Sec. 3.3. However, these initially chosen impedance parameters should be modified to guarantee the absolute stability (by satisfying (47)) if communication delays exist in the system. To

specify these required modifications, the partial derivatives of $\beta_5(\omega)$ with respect to the impedance parameters are obtained using Eq. (47) as

$$\frac{\partial \beta_5(\omega)}{\partial b_{imp_m}} = b_{imp_s}\omega^2 \Big/ \left(b_{imp_s}^2\omega^2 + \left(k_{imp_s} - m_{imp_s}\omega^2\right)^2 \right) \tag{48}$$

$$\frac{\partial \beta_5(\omega)}{\partial k_{imp_s}} = \frac{2b_{imp_m}b_{imp_s}\omega^2\left(m_{imp_s}\omega^2 - k_{imp_s}\right)}{\left(b_{imp_s}^2\omega^2 + \left(k_{imp_s} - m_{imp_s}\omega^2\right)^2 \right)^2} \tag{49}$$

$$\frac{\partial \beta_5(\omega)}{\partial b_{imp_s}} = \frac{b_{imp_m}\omega^2\left(-b_{imp_s}^2\omega^2 + \left(k_{imp_s} - m_{imp_s}\omega^2\right)^2\right)}{\left(b_{imp_s}^2\omega^2 + \left(k_{imp_s} - m_{imp_s}\omega^2\right)^2 \right)^2} \tag{50}$$

$$\frac{\partial \beta_5(\omega)}{\partial m_{imp_s}} = \frac{2b_{imp_m}b_{imp_s}\omega^4\left(k_{imp_s} - m_{imp_s}\omega^2\right)}{\left(b_{imp_s}^2\omega^2 + \left(k_{imp_s} - m_{imp_s}\omega^2\right)^2 \right)^2} \tag{51}$$

Thus, if inequality (47) is not satisfied ($\beta_5(\omega) < 0$) in some frequency ranges using the initially chosen parameters, Eqs. (48)-(51) will help the designer to increase the value of stability index $\beta_5(\omega)$ by modifying the impedance parameters (b_{imp_m} , k_{imp_s} , b_{imp_s} and m_{imp_s}) until inequality (47) is satisfied for different frequencies. Accordingly, the frequency intervals in which the decrease of each impedance parameter will increase the value of $\beta_5(\omega)$ (when $\partial\beta_5/\partial p$ is negative) and improve the stability of trilateral tele-haptic system are determined using Eqs. (48)-(51) and listed in Table 1.

Based on Table 1, the stability will be improved in low, moderate and high frequencies by reductions in k_{imp_s} , b_{imp_s} and m_{imp_s} , respectively. However, decrease of these slave impedance parameters weakens the position synchronization performance as described in Sec. 3.3. Also, the stability index $\beta_5(\omega)$ increases in all frequencies with

an increase in the master damping b_{imp_m} according to Table 1; however, it may weaken the force reflection performance during high velocity motions as discussed in Sec. 3.3.

Therefore, the position synchronization and force reflection performances (generally, the transparency of tele-haptic system) may be attenuated by revising the impedance parameters in order to ensure the absolute stability in the presence of communication delays. This indicates a trade-off between the transparency and the required absolute stability of delayed trilateral teleperation systems using the proposed impedance controller (i.e., the TMRAIC scheme).

6. EXPERIMENTAL STUDIES

The proposed trilateral impedance-based control strategy is evaluated by some experiments on two 3-DOF Phantom Premium robots (Geomagic Inc., Wilmington, MA, USA) as the masters (Fig. 3a) and one 2-DOF Quanser robot (Quanser Consulting Inc., Markham, ON, Canada) as the slave (Fig. 3b), all with nonlinear dynamics. The Phantom robots 1 and 2 are respectively equipped with a 6-axis JR3 50M31 force/torque sensor (JR3 Inc., Woodland, CA, USA) and a 6-axis ATI Nano43 force/torque sensor (ATI Industrial Automation, Apex, NC, USA) to measure the operators forces ($\mathbf{f}_{hum_1}$, $\mathbf{f}_{hum_2}$). The Quanser robot is also equipped with a 6-axis ATI Gamma F/T sensor (ATI Industrial Automation, Apex, NC, USA) to measure the applied force to the environment ($\mathbf{f}_{env}$). The proposed controller is implemented with the sampling rate of 1 *k*Hz by employing the QUARC software (Quanser Consulting Inc., Markham, ON, Canada) as a real-time control environment.

The masters and slave robots' end-effectors can move in the horizontal $x-y$ space as shown in Fig. 3. Therefore, the end-effector position of each robot is defined in the Cartesian coordinates as $\mathbf{x}_j = [x \quad y]_j^T$ (for $j = m_1, m_2, s$). A stiff environment is prepared by a set of springs (Fig. 3b) that physically interacts with the slave robot. The kinematics and dynamics of the Phantom and Quanser robots were comprehensively described in [50] and [51, 52], which are not mentioned here for the brevity. The parameters of the designed control laws (15)-(17) and adaptation laws (35) in these experimental evaluations are listed in Table 2. The function $\mathrm{sgn}(\mathbf{s}_s)$ in the slave control law (17) is replaced by the continuous alternative function of $\tanh(160\mathbf{s}_s)$ to prevent from undesired discontinuities and chattering in the applied control forces.

6.1. Without Communication Delays

In the first part of experiments, the communication channels between the masters and slave are delay-free ($T_1 = T_2 = 0$). According to the absolute stability analysis of the proposed controlled system in Sec. 5, the parameters values of the impedance models (7) and (8) should be only positive. Moreover, to provide the transparency condition (simultaneous force reflection and position synchronization), the masters impedance parameters should be small and the slave impedance parameters should be large as discussed in Sec. 3.3. Accordingly, the employed impedance parameters for the delay-free case are mentioned in Table 3. Due to the similar workspaces of the masters (Phantom robots) and the slave (Quanser robot) in planar motions, the position scaling factor is considered to be $\eta_{\mathrm{x}} = 1$. The force scaling factor is also chosen $\eta_{\mathrm{f}} = 1/2$ in order

to have two times larger environment force ($\mathbf{f}_{env}$) in comparison with the sum of scaled human operators forces ($\alpha_{\mathrm{f}}\mathbf{f}_{hum_1} + (1-\alpha_{\mathrm{f}})\mathbf{f}_{hum_2}$). Two different cases of the authority factors (α_{f}, α_{x}) are employed in these experiments as listed in Table 3.

6.1.1. Case 1: With the same authority for Operators 1 and 2

As the first case of delay-free teleoperation, the position and force authority factors are set as $\alpha_{\mathrm{f}} = \alpha_{\mathrm{x}} = 0.5$ in order to provide the same authority for the Operators 1 and 2 to manipulate robots. For this case, the position trajectory of the masters and slave robots' end-effectors with the desired responses of the master and slave reference impedance models (7) and (8) in x direction are shown in Fig. 4a. The position tracking errors between robots and their desired impedance response ($\tilde{\mathbf{x}}_{m_1}$, $\tilde{\mathbf{x}}_{m_2}$, $\tilde{\mathbf{x}}_s$) and between the masters and slave robots $\mathbf{x}_s - \eta_{\mathrm{x}}(\alpha_{\mathrm{x}}\mathbf{x}_{m_1} + (1-\alpha_{\mathrm{x}})\mathbf{x}_{m_2})$ are shown in Fig. 4b.

Considering Fig. 4, the position tracking performance between each robot and its desired reference impedance trajectory ($\tilde{\mathbf{x}}_{m_1} \to 0$, $\tilde{\mathbf{x}}_{m_2} \to 0$, $\tilde{\mathbf{x}}_s \to 0$) is obtained as a result of the proposed nonlinear TMRAIC scheme, which was proven in Sec. 4.3 via the Lyapunov method. Moreover, the position difference between the masters and the slave robots ($\mathbf{x}_s - \eta_{\mathrm{x}}(\alpha_{\mathrm{x}}\mathbf{x}_{m_1} + (1-\alpha_{\mathrm{x}})\mathbf{x}_{m_2})$) remains small (less than 0.0007 m) after the convergence of position tracking errors in the proposed teleoperation system because of choosing large parameters (m_{imp_s}, b_{imp_s} and k_{imp_s}) for the slave impedance model (8), as described in Sec. 3.3. However, this masters-slave position difference does not

converge exactly to the zero whenever there is a non-zero environment force $\mathbf{f}_{env}$ based on (8) and (9).

The interaction forces applied from the human operators to the masters ($\mathbf{f}_{hum_1}$ and $\mathbf{f}_{hum_2}$), the scaled combination of these forces ($\alpha_{\mathrm{f}}\mathbf{f}_{hum_1} + (1-\alpha_{\mathrm{f}})\mathbf{f}_{hum_2}$) and the scaled interaction force applied from the slave to the stiff environment ($\eta_{\mathrm{f}}\mathbf{f}_{env}$) in x direction are shown in Fig. 5a. The force reflection error as the difference of operators' and environment's forces ($\alpha_{\mathrm{f}}\mathbf{f}_{hum_1} + (1-\alpha_{\mathrm{f}})\mathbf{f}_{hum_2} - \eta_{\mathrm{f}}\mathbf{f}_{env}$) is also illustrated in Fig. 5b, which is less than $0.14\ \mathrm{N}$. As seen, the force reflection performance is achieved because of choosing small parameters (m_{imp_m} and b_{imp_m} in Table 3) for the master impedance model (7), which is discussed in Sec. 3.3.

In this case, the magnitude of scaled forces of the operators 1 and 2 are similar for approximately the same movements, by considering the same authority for them.

6.1.2. Case 2: With higher authority for Operator 1

In the second case, the proposed trilateral impedance-based controller is evaluated when a higher authority ($\alpha_{\mathrm{f}} = \alpha_{\mathrm{x}} = 0.8$) is considered for the operator 1 in comparison with the operator 2 (that has $(1-\alpha_{\mathrm{f}}) = (1-\alpha_{\mathrm{x}}) = 0.2$ authority). As shown in Fig. 6 (for y direction), the position synchronization and force reflection performances are achieved due to the appropriate masters and slave impedance adjustments, similar to the previous case. The sequence and duration of applying the force by the operators 1 and 2 are expressed in Fig. 6.

As seen in Fig. 6b, the applied force by the operator 2 that was multiplied by $(1-\alpha_f)=0.2$ has four times smaller authority in comparison with the force of operator 1 multiplied by $\alpha_f=0.8$. Similar to the presented results in Sec. 6.1, the transparency condition (position synchronization plus force reflection) was provided appropriately for the nonlinear trilateral tele-haptic system using the nonlinear TMRAIC control scheme. This condition is achieved in this part of experiments via the arbitrary adjustment of positive impedance parameters due to the absence of communication delays ($T_1=T_2=0$) as discussed in Sec. 5.

6.2. With Communication Delays

In this part of experiments, the proposed controller is evaluated in the presence of bounded time delays in the communication channels. In this condition, the trilateral teleoperation system should become robust against the upper bounds of communication delays that are considered to be $T_1=70\ m\sec$ and $T_2=70\ m\sec$. This assumption is due to the fact that the coast-to-coast round trip communication delays are usually in the order of 60 msec [1]. As discussed in Sec. 5, the inequality (47) for the absolute stability index $\beta_5(\omega)$ may not hold for every arbitrary set of positive impedance parameters.

As a result, the mentioned parameters in Table 3 for delay-free condition (provided the transparency) should be modified based on the guidelines presented in Sec. 5.1 in order to guarantee the trilateral absolute stability of the system. The modified impedance parameters that satisfy inequality (47) of the stability index $\beta_5(\omega)$

in working frequencies are listed in Table 4. The force and position scaling factors (η_{f}, η_{x}) are not changed in order to have the same ratio of interaction forces as the delay-free teleoperation (Sec. 6.1) and due to the same robots' workspaces.

Figure 7 shows the positive value of the absolute stability index β_5 for a wide range of frequencies by employing the modified impedance parameters (Table 4), which demonstrates the satisfaction of (47).

6.2.1. Case 1: With the same authority for Operators 1 and 2

As shown in Fig. 8a for $\alpha_{\mathrm{f}} = \alpha_{\mathrm{x}} = 0.5$, the combination of human operators' interaction forces $\alpha_{\mathrm{f}}\mathbf{f}_{hum_1} + (1-\alpha_{\mathrm{f}})\mathbf{f}_{hum_2}$ is a little different from the scaled environment force $\eta_{\mathrm{f}}\mathbf{f}_{env}$, especially during the motion when the robots' velocities are not zero. This force reflection error (Fig. 8b) is due to the increase of modified damping coefficient b_{imp_m} in the master impedance model (7) for the absolute stability guarantee. As a result, the maximum force reflection error in this case (0.6 N) is about 4 times larger than the maximum error (0.14 N) obtained in the previous delay-free experiments (Fig. 5). However, in stationary positions when the robots have approximately zero velocities and accelerations, the force reflection error becomes zero ($\alpha_{\mathrm{f}}\mathbf{f}_{hum_1} + (1-\alpha_{\mathrm{f}})\mathbf{f}_{hum_2} - \eta_{\mathrm{f}}\mathbf{f}_{env}) \to 0$, which is in accordance with Eq. (7).

Note that the high-frequency variation of force reflection errors shown in Figs. 5b and 8b is due to the variation of human operators' forces ($\mathbf{f}_{hum_1}$ and $\mathbf{f}_{hum_2}$). These variations (which have the amplitude of about 0.05 N in Figs. 5b and 8b) are less than 3 % of the maximum total force of each operator that is about 2.2 N in Figs. 5a and 8a.

This behavior is due to the human operators' force regulation performance during their hand motions and interaction with the master robots.

In addition, due to the modification and decrease of the slave impedance parameters (k_{imp_s}, b_{imp_s} and m_{imp_s} in Table 4), the remaining maximum position error (0.007 m in Fig. 9) of the slave robot with respect to the master robots becomes about 10 times larger in comparison with the previous experiments (illustrated in Fig. 4) without time delay.

6.2.2. Case 2: With higher authority for Operator 1

The force and position data when the higher authority is considered for the operator 1 in comparison with the operator 2 using $\alpha_{\mathrm{f}} = \alpha_{\mathrm{x}} = 0.8$ and the upper bounds of communication delays are $T_1 = 70\ m\mathrm{sec}$ and $T_2 = 70\ m\mathrm{sec}$, are shown in Fig. 10a and 10b, respectively (for y direction). As seen, the operator 2 applies larger forces to move the robots in comparison with the operator 1 because of the smaller authority $(1-\alpha_{\mathrm{f}}) = 0.2$ of operator 2 in this case.

According to the obtained results for the proposed trilateral controller in the presence of communication delays (Sec. 6.2), the force reflection performance (Figs. 8 and 10a), the position synchronization performance (Figs. 9 and 10b) and consequently the transparency of teleoperation system are affected by the required modifications to the impedance parameters; however, the absolute stability is ensured. This implies a trade-off between the absolute stability and the transparency in the proposed trilateral system that was introduced in Sec. 5.1.

As discussed before, the time delays (T_1, T_2) of real communication channels are usually close to constant and do not change very much during a teleoperation task and an upper bound of delay can be considered as the worst case which can be estimated by comparing the sending and receiving times of transmitted signals [45]. The performance of the proposed trilateral control strategy with the compensation of highly varying time delays will be studied in future works.

5. CONCLUSION

In this paper, a new nonlinear Trilateral Model Reference Adaptive Impedance Controller (TMRAIC) was presented and tested for nonlinear dual-user multi-DOF teleoperation systems including two masters and one slave robots. The proposed controller provided the position synchronization and the force reflection by implementing two reference impedance models and adjusting their parameters. These impedance parameters were employed in trilateral control laws to make the closed-loop dynamics of robots similar to their corresponding reference impedance models. The tracking convergence to the reference models' responses in the presence of parametric uncertainties were proven via the Lyapunov method and evaluated experimentally.

The trilateral absolute stability of the teleoperation system was also guaranteed for the first time by adjusting the desired impedance parameters in the presence of communication delays, without assuming any reduction to a two-port network. A trade-off between the absolute stability and transparency of the three-port system subjected to time delays should be applied using the proposed TMRAIC scheme. The experimental

studies employing multi-DOF nonlinear masters and slave robots, demonstrated that the position and force tracking performances and the teleoperation system's stability were achieved with and without communication delays.

REFERENCES

[1] Nudehi, S. S., Mukherjee, R., and Ghodoussi, M., 2005, "A Shared-Control Approach to Haptic Interface Design for Minimally Invasive Telesurgical Training," IEEE Transactions on Control Systems Technology, 13(4), pp. 588-592.
[2] Shamaei, K., Kim, L. H., and Okamura, A. M., 2015, "Design and Evaluation of a Trilateral Shared-Control Architecture for Teleoperated Training Robots," International Conference of the IEEE Engineering in Medicine and Biology Society (EMBC), pp. 4887-4893.
[3] Carignan, C. R., and Olsson, P. A., 2004, "Cooperative Control of Virtual Objects over the Internet Using Force-Reflecting Master Arms," IEEE International Conference on Robotics and Automation (ICRA), pp. 1221-1226.
[4] Gupta, A., and O'malley, M. K., 2006, "Design of a Haptic Arm Exoskeleton for Training and Rehabilitation," IEEE/ASME Transactions on Mechatronics, 11(3), pp. 280-289.
[5] Malysz, P., and Sirouspour, S., 2009, "Dual-Master Teleoperation Control of Kinematically Redundant Robotic Slave Manipulators," IEEE/RSJ International Conference on Intelligent Robots and Systems (IROS), pp. 5115-5120.
[6] Colgate, J. E., 1993, "Robust Impedance Shaping Telemanipulation," IEEE Transactions on Robotics and Automation, 9(4), pp. 374-384.
[7] Dongjun, L., and Li, P. Y., 2003, "Passive Bilateral Feedforward Control of Linear Dynamically Similar Teleoperated Manipulators," IEEE Transactions on Robotics and Automation, 19(3), pp. 443-456.
[8] Lawrence, D. A., 1993, "Stability and Transparency in Bilateral Teleoperation," IEEE Transactions on Robotics and Automation, 9(5), pp. 624-637.
[9] Yokokohji, Y., and Yoshikawa, T., 1994, "Bilateral Control of Master-Slave Manipulators for Ideal Kinesthetic Coupling-Formulation and Experiment," IEEE Transactions on Robotics and Automation, 10(5), pp. 605-620.
[10] Polushin, I. G., Liu, P. X., Lung, C.-H., and On, G. D., 2010, "Position-Error Based Schemes for Bilateral Teleoperation with Time Delay: Theory and Experiments," Journal of Dynamic Systems, Measurement, and Control, 132(3), pp. 031008 (11 pages).
[11] Lee, H. K., and Chung, M. J., 1998, "Adaptive Controller of a Master–Slave System for Transparent Teleoperation," Journal of Robotic Systems, 15(8), pp. 465-475.
[12] Shi, M., Tao, G., and Liu, H., 2002, "Adaptive Control of Teleoperation Systems," Journal of X-Ray Science and Technology, 10(1-2), pp. 37-57.
[13] Wen-Hong, Z., and Salcudean, S. E., 2000, "Stability Guaranteed Teleoperation: An Adaptive Motion/Force Control Approach," IEEE Transactions on Automatic Control, 45(11), pp. 1951-1969.

[14] Malysz, P., and Sirouspour, S., 2009, "Nonlinear and Filtered Force/Position Mappings in Bilateral Teleoperation with Application to Enhanced Stiffness Discrimination," IEEE Transactions on Robotics, 25(5), pp. 1134-1149.
[15] Lee, D., and Spong, M. W., 2006, "Passive Bilateral Teleoperation with Constant Time Delay," IEEE Transactions on Robotics, 22(2), pp. 269-281.
[16] Chopra, N., Spong, M. W., and Lozano, R., 2008, "Synchronization of Bilateral Teleoperators with Time Delay," Automatica, 44(8), pp. 2142-2148.
[17] Nuño, E., Ortega, R., and Basañez, L., 2010, "An Adaptive Controller for Nonlinear Teleoperators," Automatica, 46(1), pp. 155-159.
[18] Liu, Y. C., and Chopra, N., 2013, "Control of Semi-Autonomous Teleoperation System with Time Delays," Automatica, 49(6), pp. 1553-1565.
[19] Ryu, J. H., and Kwon, D. S., 2001, "A Novel Adaptive Bilateral Control Scheme Using Similar Closed-Loop Dynamic Characteristics of Master/Slave Manipulators," Journal of Robotic Systems, 18(9), pp. 533-543.
[20] Liu, X., and Tavakoli, M., 2012, "Adaptive Control of Teleoperation Systems with Linearly and Nonlinearly Parameterized Dynamic Uncertainties," Journal of Dynamic Systems, Measurement, and Control, 134(2), pp. 021015 (10 pages).
[21] Sharifi, M., Behzadipour, S., and Salarieh, H., 2016, "Nonlinear Bilateral Adaptive Impedance Control with Applications in Telesurgery and Telerehabilitation," Journal of Dynamic Systems, Measurement, and Control, 138(11), pp. 111010 (16 pages).
[22] Lo, W., Liu, Y., Elhajj, I. H., Xi, N., Wang, Y., and Fukuda, T., 2004, "Cooperative Teleoperation of a Multirobot System with Force Reflection Via Internet," IEEE/ASME Transactions on Mechatronics, 9(4), pp. 661-670.
[23] Katsura, S., Matsumoto, Y., and Ohnishi, K., 2005, "Realization of "Law of Action and Reaction" by Multilateral Control," IEEE Transactions on Industrial Electronics, 52(5), pp. 1196-1205.
[24] Katsura, S., and Ohnishi, K., 2006, "A Realization of Haptic Training System by Multilateral Control," IEEE Transactions on Industrial Electronics, 53(6), pp. 1935-1942.
[25] Sirouspour, S., 2005, "Modeling and Control of Cooperative Teleoperation Systems," IEEE Transactions on Robotics, 21(6), pp. 1220-1225.
[26] Moghimi, S., Sirouspour, S., and Malysz, P., 2008, "Haptic-Enabled Collaborative Training with Generalized Force and Position Mappings," Symposium on Haptic Interfaces for Virtual Environment and Teleoperator Systems, pp. 287-294.
[27] Gueaieb, W., Karray, F., and Al-Sharhan, S., 2007, "A Robust Hybrid Intelligent Position/Force Control Scheme for Cooperative Manipulators," IEEE/ASME Transactions on Mechatronics, 12(2), pp. 109-125.
[28] Khademian, B., and Hashtrudi-Zaad, K., 2012, "Dual-User Teleoperation Systems: New Multilateral Shared Control Architecture and Kinesthetic Performance Measures," IEEE/ASME Transactions on Mechatronics, 17(5), pp. 895-906.
[29] Khademian, B., Apkarian, J., and Hashtrudi-Zaad, K., 2011, "Assessment of Environmental Effects on Collaborative Haptic Guidance," Presence: Teleoperators & Virtual Environments, 20(3), pp. 191-206.
[30] Wang, Y., Sun, F., Liu, H., and Li, Z., 2010, "Passive Four-Channel Multilateral Shared Control Architecture in Teleoperation," IEEE International Conference on Cognitive Informatics (ICCI), pp. 851-858.

[31] Mendez, V., and Tavakoli, M., 2010, "A Passivity Criterion for N-Port Multilateral Haptic Systems," IEEE Conference on Decision and Control (CDC), pp. 274-279.
[32] Panzirsch, M., Artigas, J., Tobergte, A., Kotyczka, P., Preusche, C., Albu-Schaeffer, A., and Hirzinger, G., 2012, Haptics: Perception, Devices, Mobility, and Communication: International Conference, Eurohaptics. Proceedings, Part I, Springer Berlin Heidelberg, Berlin, Heidelberg, A Peer-to-Peer Trilateral Passivity Control for Delayed Collaborative Teleoperation.
[33] Hashemzadeh, F., Sharifi, M., and Tavakoli, M., 2016, "Nonlinear Trilateral Teleoperation Stability Analysis Subjected to Time-Varying Delays," Control Engineering Practice, 56(pp. 123-135.
[34] Li, J., Tavakoli, M., Mendez, V., and Huang, Q., 2015, "Passivity and Absolute Stability Analyses of Trilateral Haptic Collaborative Systems," Journal of Intelligent & Robotic Systems, 78(1), pp. 3-20.
[35] Shahbazi, M., Atashzar, S. F., Talebi, H. A., and Patel, R. V., 2015, "Novel Cooperative Teleoperation Framework: Multi-Master/Single-Slave System," IEEE/ASME Transactions on Mechatronics, 20(4), pp. 1668-1679.
[36] Kuo, R. F., and Chu, T. H., 2010, "Unconditional Stability Boundaries of a Three-Port Network," IEEE Transactions on Microwave Theory and Techniques, 58(2), pp. 363-371.
[37] Khademian, B., and Hashtrudi-Zaad, K., 2011, "Shared Control Architectures for Haptic Training: Performance and Coupled Stability Analysis," International Journal of Robotics Research, 30(13), pp. 1627-1642.
[38] Khademian, B., and Hashtrudi-Zaad, K., 2013, "A Framework for Unconditional Stability Analysis of Multimaster/Multislave Teleoperation Systems," IEEE Transactions on Robotics, 29(3), pp. 684-694.
[39] Haykin, S. S., 1970, *Active Network Theory*, Addison-Wesley Pub. Co.,
[40] Li, J., Tavakoli, M., and Huang, Q., 2014, "Absolute Stability of a Class of Trilateral Haptic Systems," IEEE Transactions on Haptics, 7(3), pp. 301-310.
[41] Sharifi, M., Behzadipour, S., and Vossoughi, G., 2014, "Nonlinear Model Reference Adaptive Impedance Control for Human–Robot Interactions," Control Engineering Practice, 32, pp. 9-27.
[42] Lu, W. S., and Meng, Q. H., 1991, "Impedance Control with Adaptation for Robotic Manipulations," Robotics and Automation, IEEE Transactions on, 7(3), pp. 408-415.
[43] Slotine, J. J. E., and Li, W., 1991, *Applied Nonlinear Control*, Prantice-Hall, NJ, Englewood Cliffs.
[44] Sharifi, M., Behzadipour, S., and Vossoughi, G. R., 2014, "Model Reference Adaptive Impedance Control in Cartesian Coordinates for Physical Human–Robot Interaction," Advanced Robotics, 28(19), pp. 1277-1290.
[45] Nuño, E., Basañez, L., and Ortega, R., 2011, "Passivity-Based Control for Bilateral Teleoperation: A Tutorial," Automatica, 47(3), pp. 485-495.
[46] Hashemzadeh, F., Hassanzadeh, I., Tavakoli, M., and Alizadeh, G., 2012, "A New Method for Bilateral Teleoperation Passivity under Varying Time Delays," Mathematical Problems in Engineering, 12(1), pp. 1-19.
[47] Haddadi, A., and Hashtrudi-Zaad, K., 2010, "Bounded-Impedance Absolute Stability of Bilateral Teleoperation Control Systems," IEEE Transactions on Haptics, 3(1), pp. 15-27.

[48] Hashtrudi-Zaad, K., and Salcudean, S. E., "Analysis of Control Architectures for Teleoperation Systems with Impedance/Admittance Master and Slave Manipulators," International Journal of Robotics Research, 20(6), pp. 419-445.
[49] Li, J., Tavakoli, M., and Huang, Q., 2014, "Absolute Stability of Multi-Dof Multilateral Haptic Systems," IEEE Transactions on Control Systems Technology, 22(6), pp. 2319-2328.
[50] Çavuşoğlu, M. C., Feygin, D., and Tendick, F., 2002, "A Critical Study of the Mechanical and Electrical Properties of the Phantom Haptic Interface and Improvements for High-Performance Control," Presence: Teleoperators & Virtual Environments, 11(6), pp. 555-568.
[51] Dyck, M. D., 2013, "Measuring the Dynamic Impedance of the Human Arm," Ph.D. thesis, University of Alberta,
[52] Dyck, M., and Tavakoli, M., 2013, "Measuring the Dynamic Impedance of the Human Arm without a Force Sensor," IEEE International Conference on Rehabilitation Robotics (ICORR), pp. 1-8.

Figure Captions List

Fig. 1 The schematic diagram of the proposed trilateral teleoperated haptic system with communication delays.

Fig. 2 The block diagram of the proposed nonlinear trilateral model reference adaptive impedance controller.

Fig. 3 Experimental system: (a) two Phantom Premium robots as the masters and (b) one Quanser robot as the slave.

Fig. 4 (a) The position trajectories of the masters ($\mathbf{x}_{m_1}$, $\mathbf{x}_{m_2}$) and slave ($\mathbf{x}_s$) with their desired reference impedance models' responses ($\mathbf{x}_{imp_m}$, $\mathbf{x}_{imp_s}$), and (b) the position tracking errors for each robot ($\tilde{\mathbf{x}}_{m_1}$, $\tilde{\mathbf{x}}_{m_2}$, $\tilde{\mathbf{x}}_s$) and between the masters and slave ($\mathbf{x}_s - \eta_{\mathrm{x}}(\alpha_{\mathrm{x}}\mathbf{x}_{m_1} + (1-\alpha_{\mathrm{x}})\mathbf{x}_{m_2})$), in x direction.

Fig. 5 (a) The operators forces $\mathbf{f}_{hum_1}$, $\mathbf{f}_{hum_2}$, sum of their scaled forces $\alpha_{\mathrm{f}}\mathbf{f}_{hum_1} + (1-\alpha_{\mathrm{f}})\mathbf{f}_{hum_2}$ and the scaled environment force $\eta_{\mathrm{f}}\mathbf{f}_{env}$, and (b) the force reflection error ($\alpha_{\mathrm{f}}\mathbf{f}_{hum_1} + (1-\alpha_{\mathrm{f}})\mathbf{f}_{hum_2} - \eta_{\mathrm{f}}\mathbf{f}_{env}$), in x direction when $\alpha_{\mathrm{f}} = \alpha_{\mathrm{x}} = 0.5$.

Fig. 6 (a) The masters and slave position trajectories ($\mathbf{x}_{m_1}$, $\mathbf{x}_{m_2}$, $\mathbf{x}_s$) with their desired reference impedance models' responses ($\mathbf{x}_{imp_m}$, $\mathbf{x}_{imp_s}$), and (b) the operators forces $\mathbf{f}_{hum_1}$, $\mathbf{f}_{hum_2}$, sum of their scaled forces

$\alpha_{\mathrm{f}}\mathbf{f}_{hum_1} + (1-\alpha_{\mathrm{f}})\mathbf{f}_{hum_2}$ and the scaled environment force $\eta_{\mathrm{f}}\mathbf{f}_{env}$, when $\alpha_{\mathrm{f}} = \alpha_{\mathrm{x}} = 0.8$ for y direction.

Fig. 7 Positiveness of the absolute stability index β_5 employing the modified impedance parameters for delayed teleoperation system.

Fig. 8 (a) The operators forces $\mathbf{f}_{hum_1}$, $\mathbf{f}_{hum_2}$, sum of their scaled forces $\alpha_{\mathrm{f}}\mathbf{f}_{hum_1} + (1-\alpha_{\mathrm{f}})\mathbf{f}_{hum_2}$ and the scaled environment force $\eta_{\mathrm{f}}\mathbf{f}_{env}$, and (b) the force reflection error ($\alpha_{\mathrm{f}}\mathbf{f}_{hum_1} + (1-\alpha_{\mathrm{f}})\mathbf{f}_{hum_2} - \eta_{\mathrm{f}}\mathbf{f}_{env}$), in x direction when $\alpha_{\mathrm{f}} = \alpha_{\mathrm{x}} = 0.5$ and the upper bounds of communication delays are $T_1 = 70\ m\sec$ and $T_2 = 70\ m\sec$.

Fig. 9 (a) The position trajectories of the masters ($\mathbf{x}_{m_1}$, $\mathbf{x}_{m_2}$) and slave ($\mathbf{x}_s$) with their desired reference impedance models' responses ($\mathbf{x}_{imp_m}$, $\mathbf{x}_{imp_s}$), and (b) the position tracking errors for each robot ($\tilde{\mathbf{x}}_{m_1}$, $\tilde{\mathbf{x}}_{m_2}$, $\tilde{\mathbf{x}}_s$) and between the masters and slave ($\mathbf{x}_s - \eta_{\mathrm{x}}(\alpha_{\mathrm{x}}\mathbf{x}_{m_1} + (1-\alpha_{\mathrm{x}})\mathbf{x}_{m_2})$), in the presence of time delays ($T_1 = 70\ m\sec$ and $T_2 = 70\ m\sec$).

Fig. 10 (a) The scaled operators $\alpha_{\mathrm{f}}\mathbf{f}_{hum_1}$, $(1-\alpha_{\mathrm{f}})\mathbf{f}_{hum_2}$ and environment $\eta_{\mathrm{f}}\mathbf{f}_{env}$ interaction forces, and (b) the masters and slave position trajectories ($\mathbf{x}_{m_1}$, $\mathbf{x}_{m_2}$, $\mathbf{x}_s$) with their desired reference impedance models' responses ($\mathbf{x}_{imp_m}$, $\mathbf{x}_{imp_s}$) in y direction, when $\alpha_{\mathrm{f}} = \alpha_{\mathrm{x}} = 0.8$ and the upper bounds of communication delays are $T_1 = 70\ m\sec$ and $T_2 = 70\ m\sec$.

Table Caption List

Table 1 Frequency intervals in which the decrease of each impedance parameter will increase the value of $\beta_5(\omega)$ ($\partial\beta_5(\omega)/\partial p < 0$)

Table 2 Parameters of control and adaptation laws used in experiments

Table 3 Parameters of impedance models (7) and (8) for the delay-free communication channels $T_1 = T_2 = 0$

Table 4 Modified impedance parameters for the absolute stability in the presence of communication delays (with the upper bounds of $T_1 = 70\ m\sec$ and $T_2 = 70\ m\sec$)

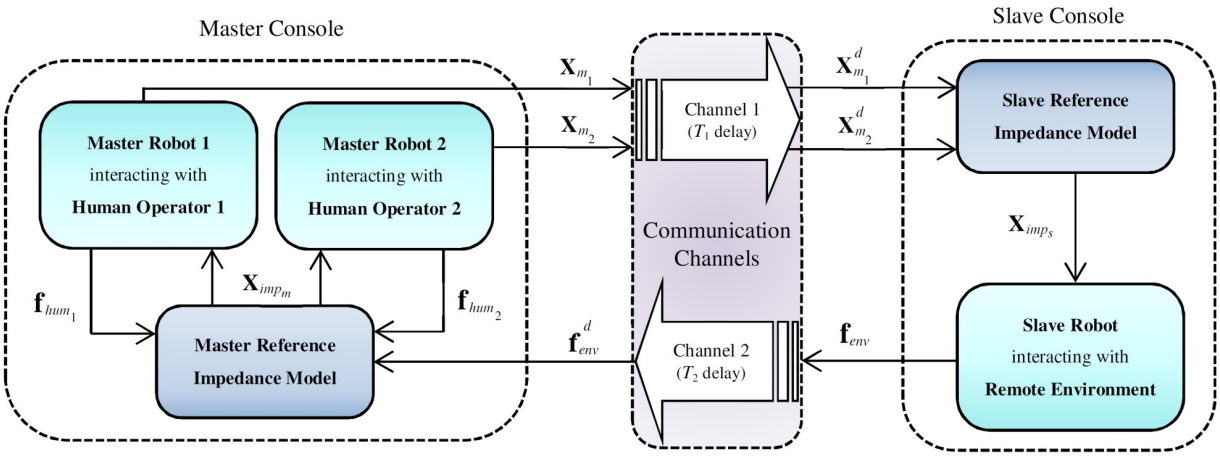

Fig. 1 The schematic diagram of the proposed trilateral teleoperated haptic system with communication delays.

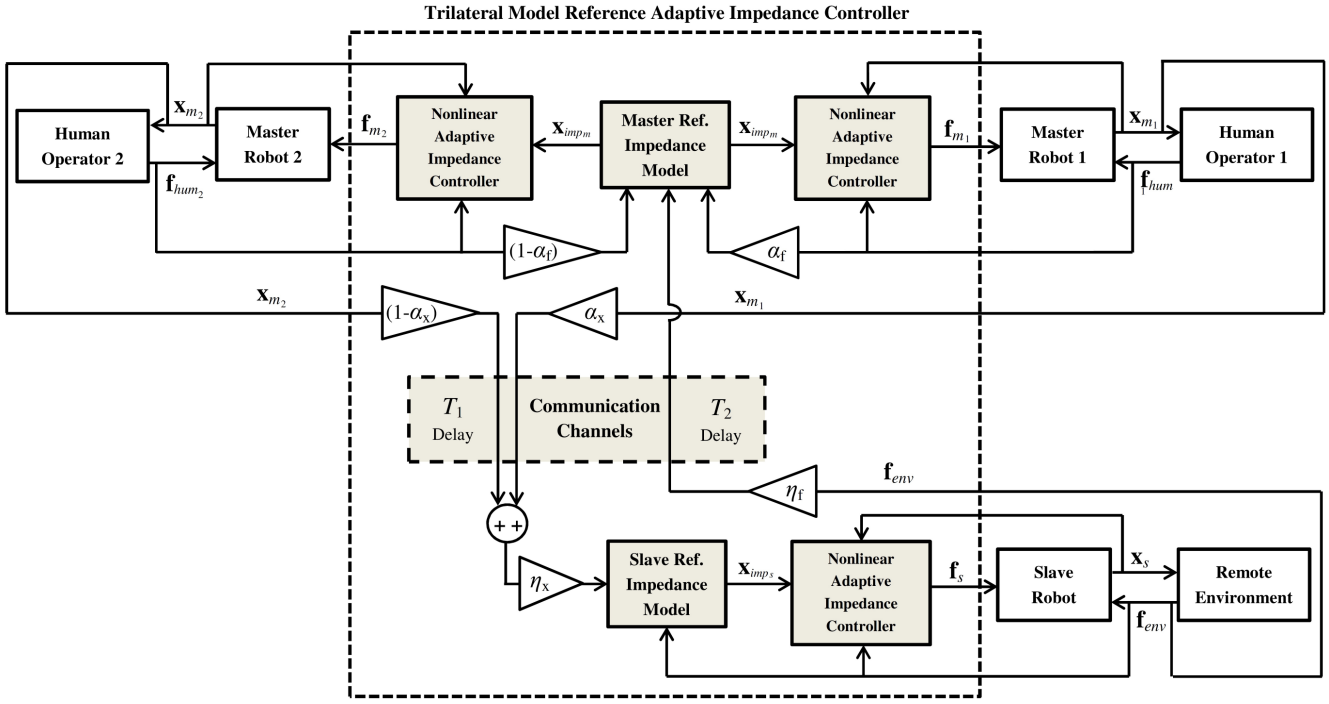

Fig. 2 The block diagram of the proposed nonlinear trilateral model reference adaptive impedance controller.

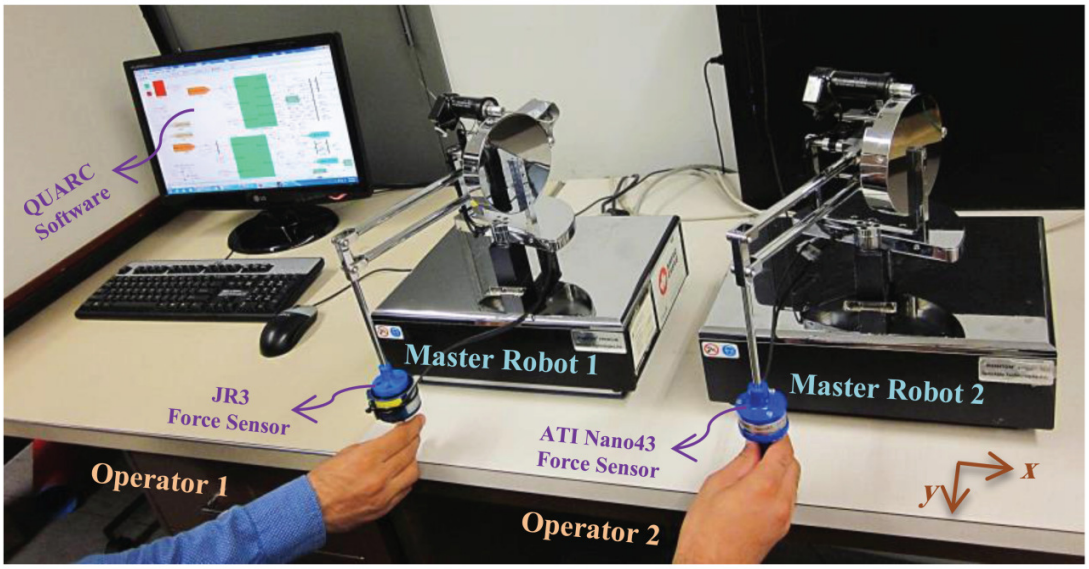

(a)

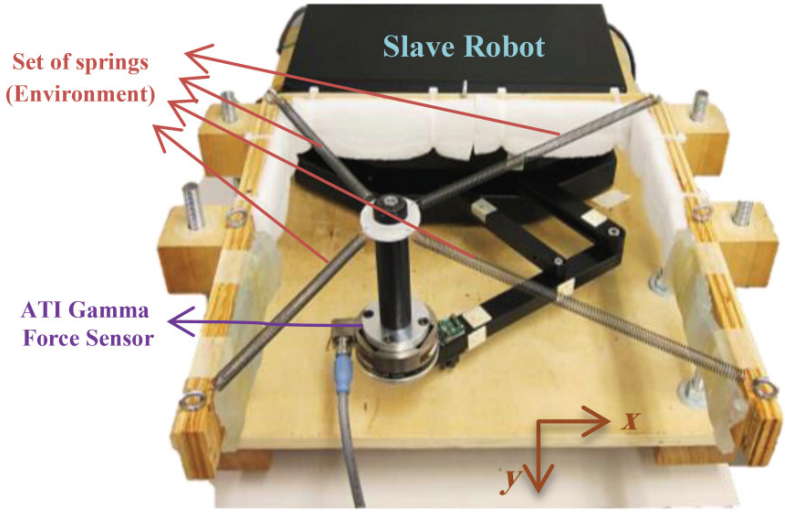

(b)

Fig. 3 Experimental system: (a) two Phantom Premium robots as the masters and (b) one Quanser robot as the slave.

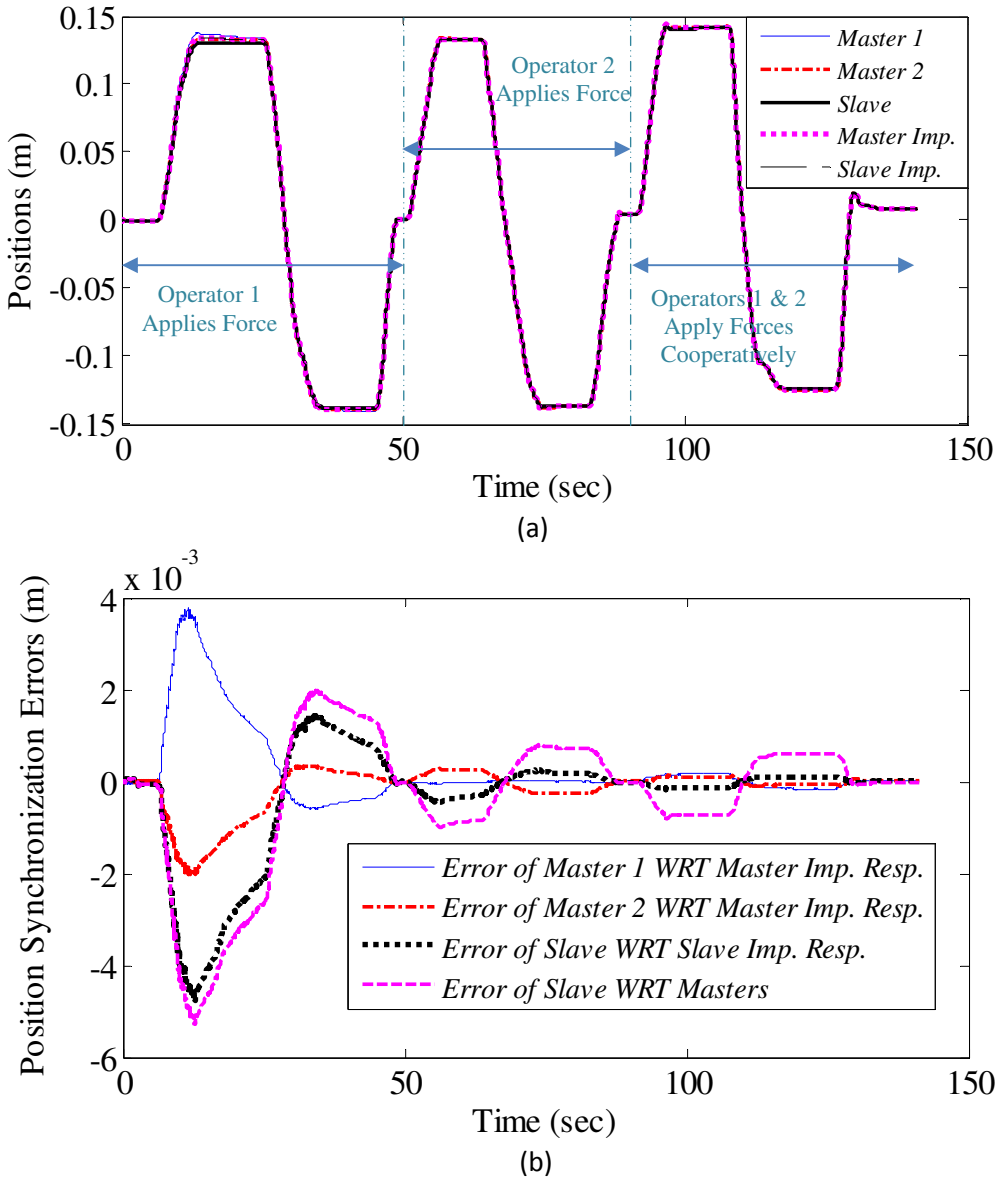

Fig. 4 (a) The position trajectories of the masters ($\mathbf{x}_{m_1}$, $\mathbf{x}_{m_2}$) and slave ($\mathbf{x}_s$) with their desired reference impedance models' responses ($\mathbf{x}_{imp_m}$, $\mathbf{x}_{imp_s}$), and (b) the position tracking errors for each robot ($\tilde{\mathbf{x}}_{m_1}$, $\tilde{\mathbf{x}}_{m_2}$, $\tilde{\mathbf{x}}_s$) and between the masters and slave ($\mathbf{x}_s - \eta_x(\alpha_x \mathbf{x}_{m_1} + (1-\alpha_x)\mathbf{x}_{m_2})$), in x direction.

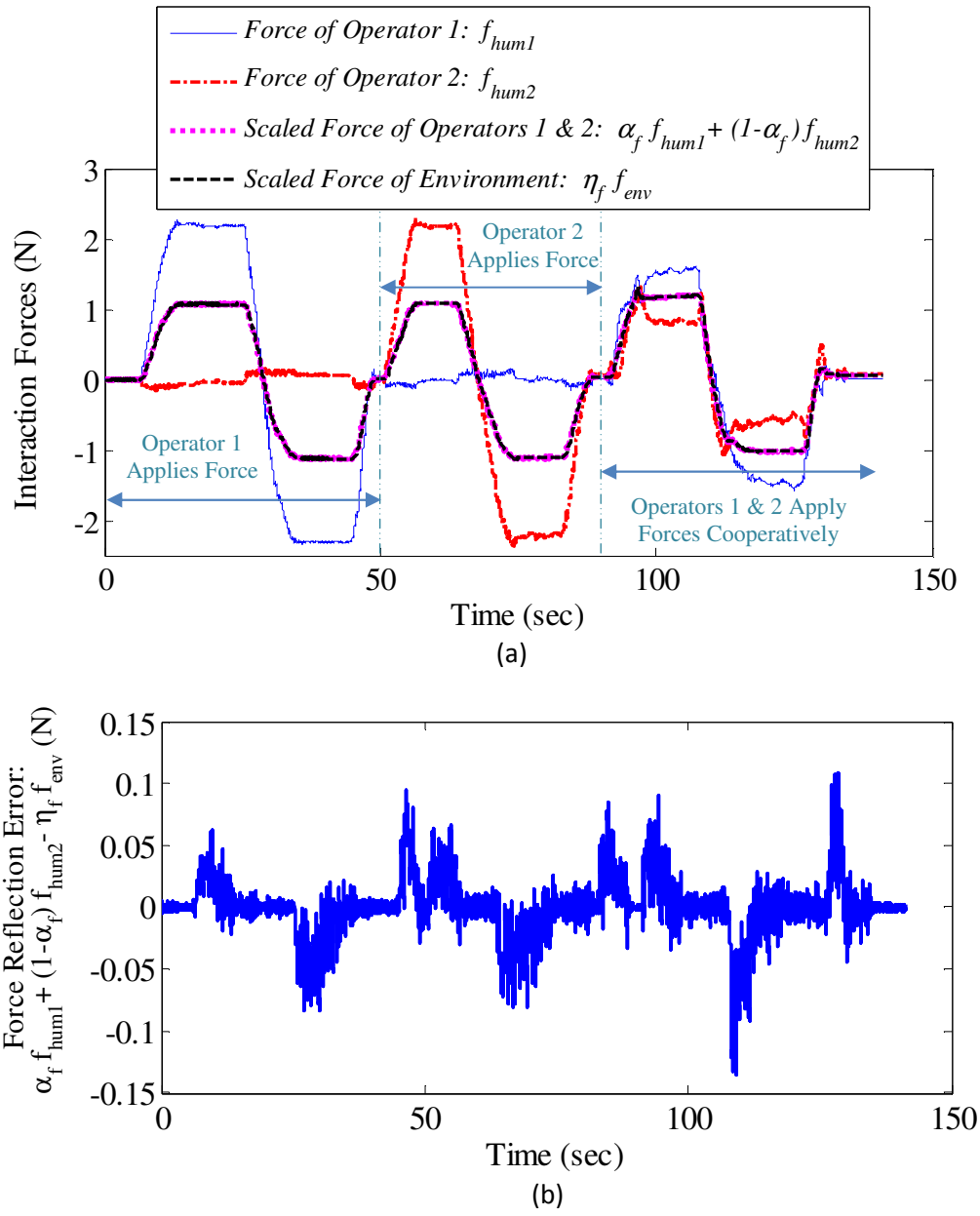

Fig. 5 (a) The operators forces $\mathbf{f}_{hum_1}$, $\mathbf{f}_{hum_2}$, sum of their scaled forces $\alpha_f \mathbf{f}_{hum_1} + (1-\alpha_f)\mathbf{f}_{hum_2}$ and the scaled environment force $\eta_f \mathbf{f}_{env}$, and (b) the force reflection error ($\alpha_f \mathbf{f}_{hum_1} + (1-\alpha_f)\mathbf{f}_{hum_2} - \eta_f \mathbf{f}_{env}$), in x direction when $\alpha_f = \alpha_x = 0.5$.

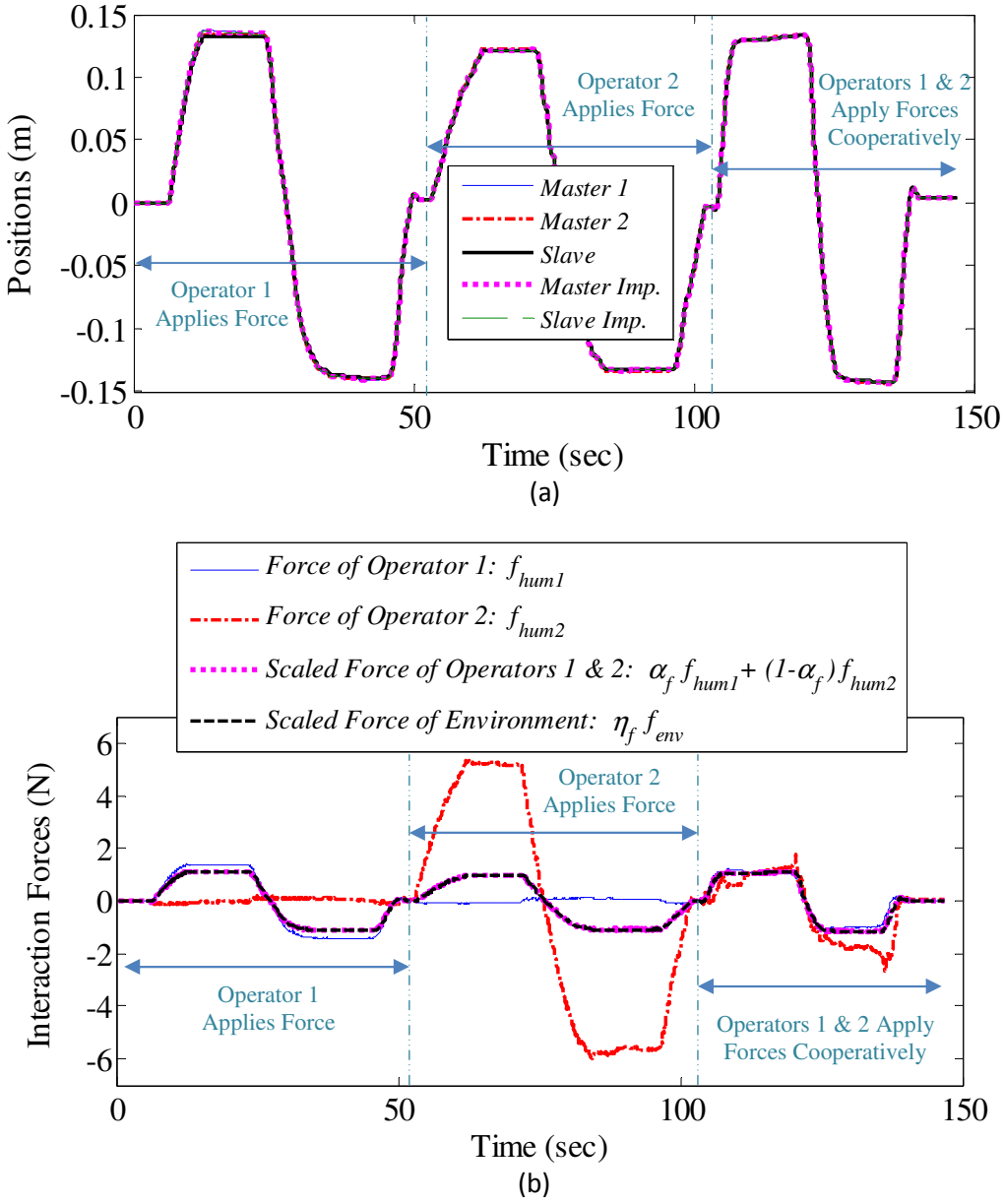

Fig. 6 (a) The masters and slave position trajectories ($\mathbf{x}_{m_1}$, $\mathbf{x}_{m_2}$, $\mathbf{x}_s$) with their desired reference impedance models' responses ($\mathbf{x}_{imp_m}$, $\mathbf{x}_{imp_s}$), and (b) the operators forces $\mathbf{f}_{hum_1}$, $\mathbf{f}_{hum_2}$, sum of their scaled forces $\alpha_f \mathbf{f}_{hum_1} + (1-\alpha_f)\mathbf{f}_{hum_2}$ and the scaled environment force $\eta_f \mathbf{f}_{env}$, when $\alpha_f = \alpha_x = 0.8$ for y direction.

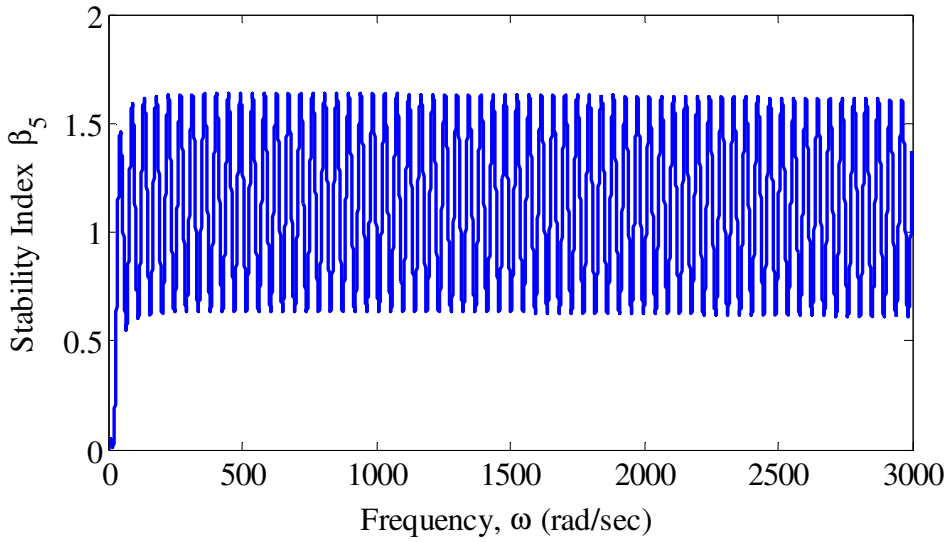

Fig. 7 Positiveness of the absolute stability index β_5 employing the modified impedance parameters for delayed teleoperation system.

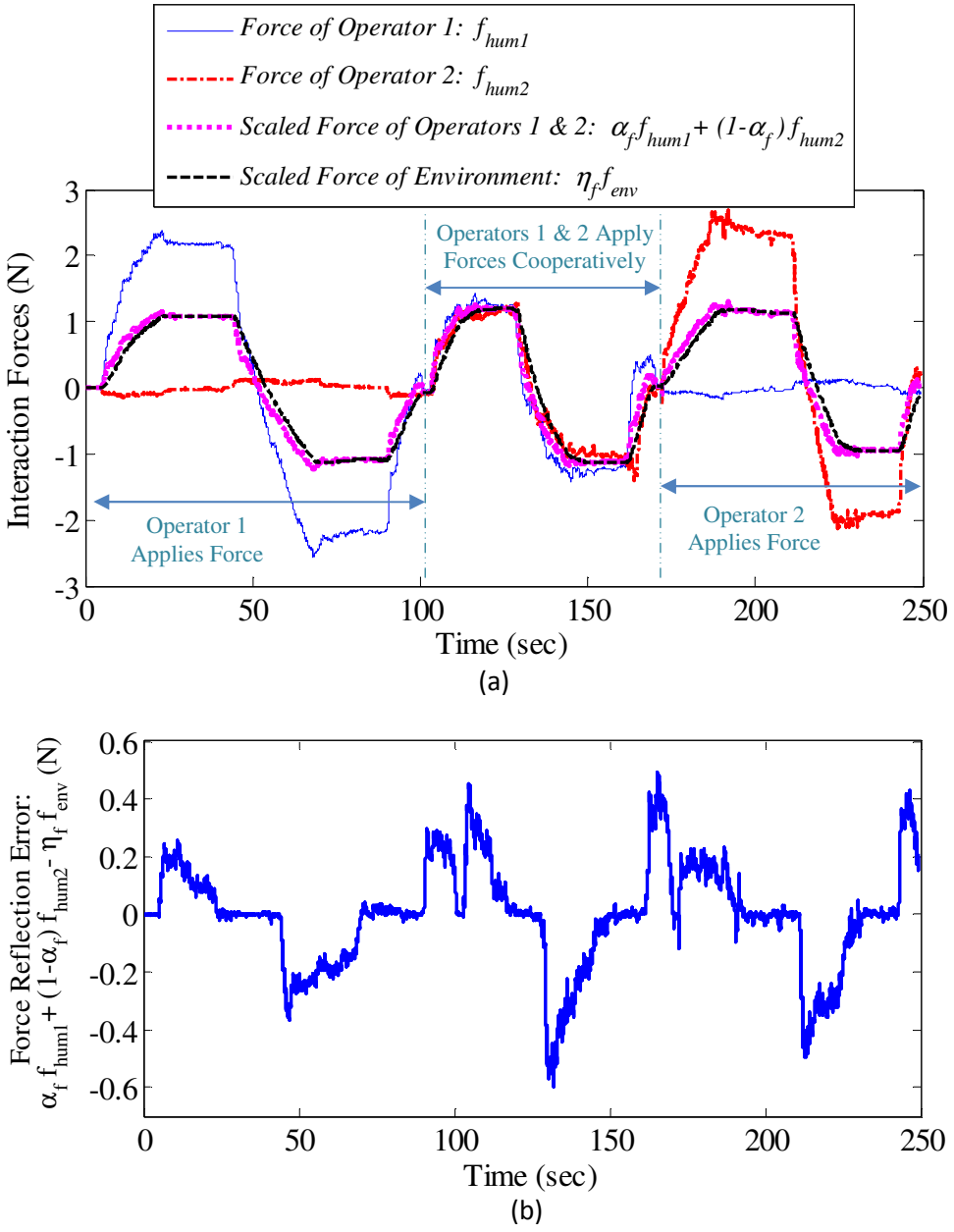

Fig. 8 (a) The operators forces $\mathbf{f}_{hum_1}$, $\mathbf{f}_{hum_2}$, sum of their scaled forces $\alpha_f \mathbf{f}_{hum_1} + (1-\alpha_f)\mathbf{f}_{hum_2}$ and the scaled environment force $\eta_f \mathbf{f}_{env}$, and (b) the force reflection error ($\alpha_f \mathbf{f}_{hum_1} + (1-\alpha_f)\mathbf{f}_{hum_2} - \eta_f \mathbf{f}_{env}$), in x direction when $\alpha_f = \alpha_x = 0.5$ and the upper bounds of communication delays are $T_1 = 70\ m\sec$ and $T_2 = 70\ m\sec$.

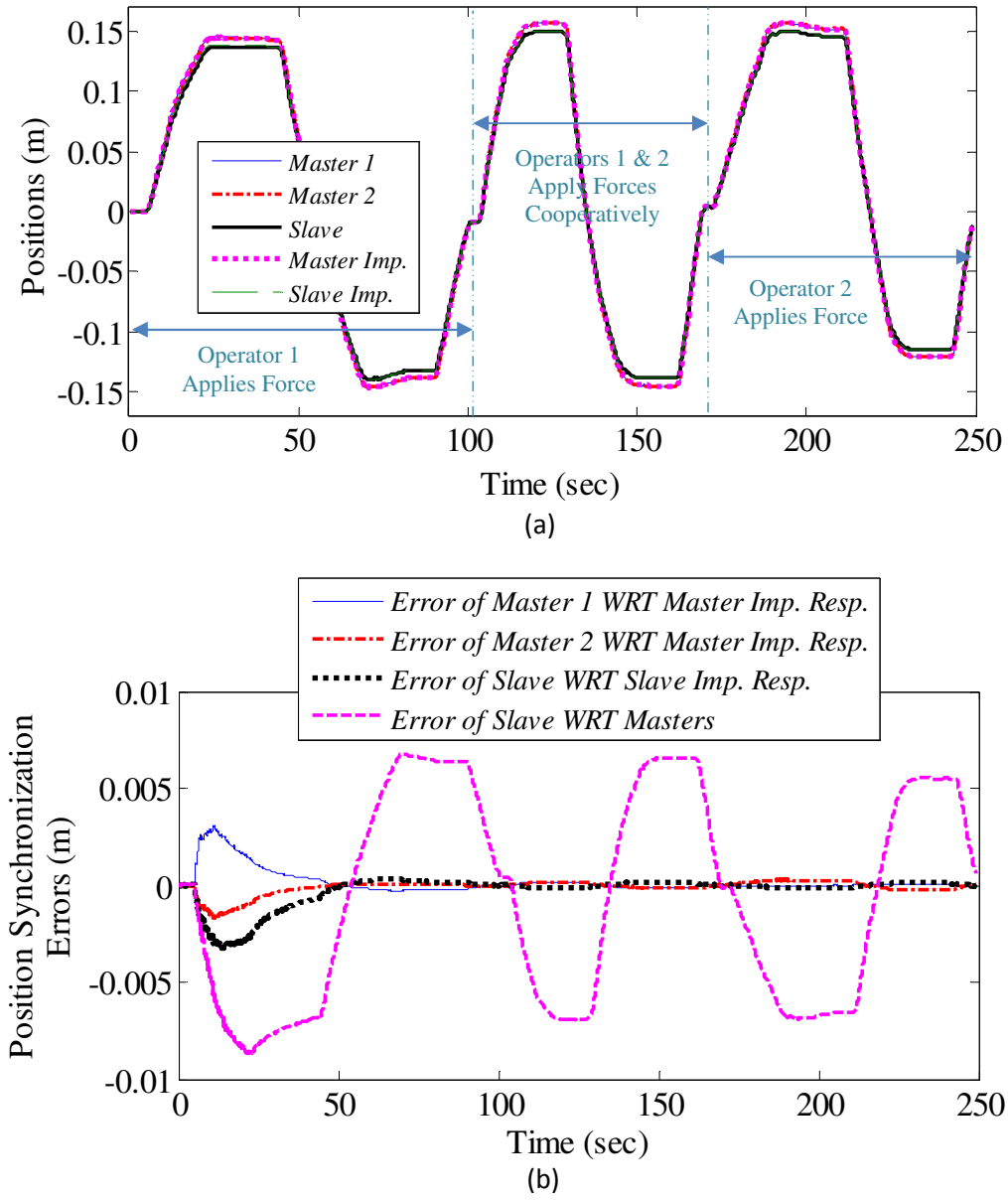

Fig. 9 (a) The position trajectories of the masters ($\mathbf{x}_{m_1}$, $\mathbf{x}_{m_2}$) and slave ($\mathbf{x}_s$) with their desired reference impedance models' responses ($\mathbf{x}_{imp_m}$, $\mathbf{x}_{imp_s}$), and (b) the position tracking errors for each robot ($\tilde{\mathbf{x}}_{m_1}$, $\tilde{\mathbf{x}}_{m_2}$, $\tilde{\mathbf{x}}_s$) and between the masters and slave ($\mathbf{x}_s - \eta_x(\alpha_x \mathbf{x}_{m_1} + (1-\alpha_x)\mathbf{x}_{m_2})$), in the presence of time delays ($T_1 = 70\ m\sec$ and $T_2 = 70\ m\sec$).

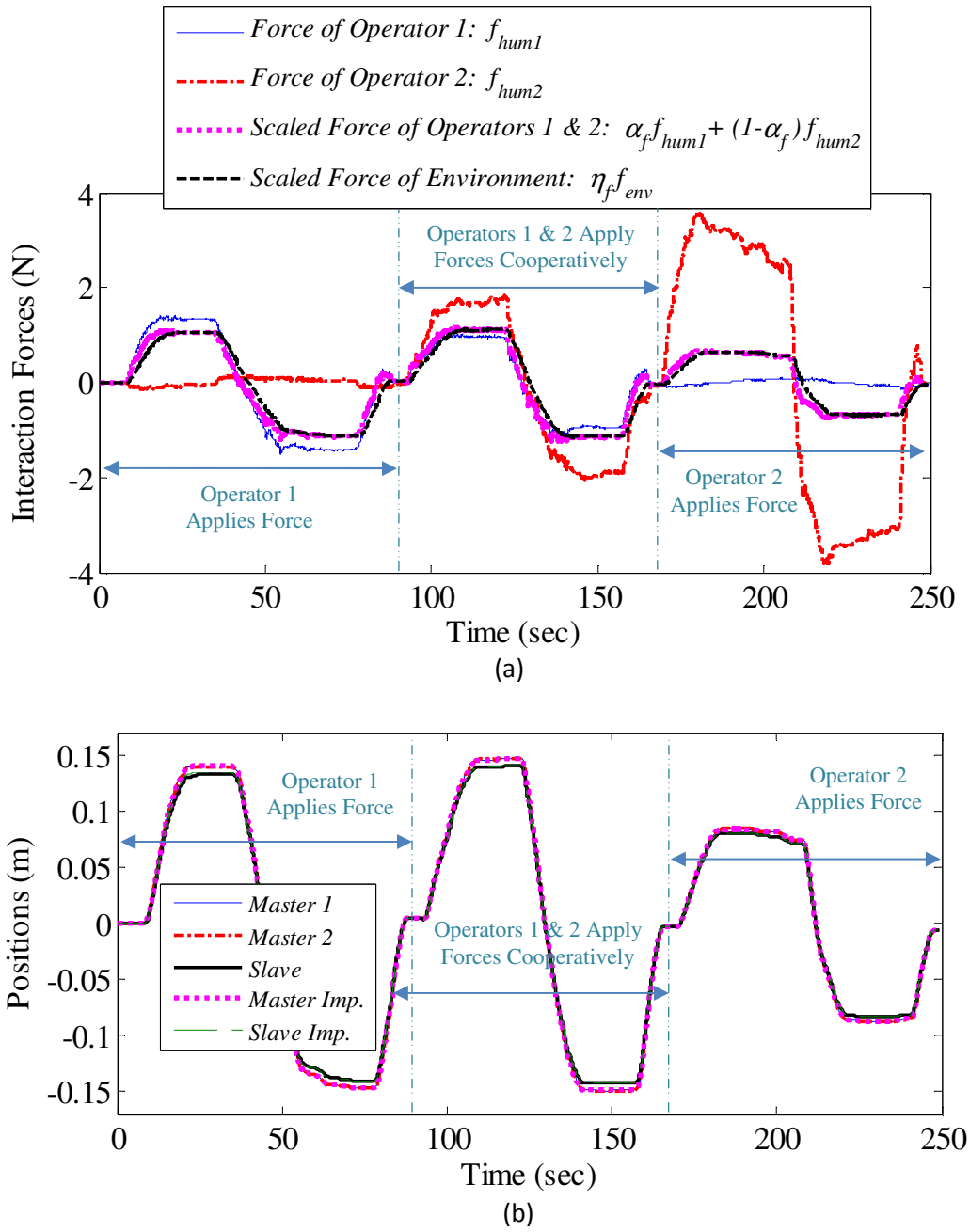

Fig. 10 (a) The scaled operators $\alpha_f \mathbf{f}_{hum_1}$, $(1-\alpha_f)\mathbf{f}_{hum_2}$ and environment $\eta_f \mathbf{f}_{env}$ interaction forces, and (b) the masters and slave position trajectories ($\mathbf{x}_{m_1}$, $\mathbf{x}_{m_2}$, $\mathbf{x}_s$) with their desired reference impedance models' responses ($\mathbf{x}_{imp_m}$, $\mathbf{x}_{imp_s}$) in y direction, when $\alpha_f = \alpha_x = 0.8$ and the upper bounds of communication delays are $T_1 = 70\ m\sec$ and $T_2 = 70\ m\sec$.

Table 1 Frequency intervals in which the decrease of each impedance parameter will increase the value of $\beta_5(\omega)$ ($\partial\beta_5(\omega)/\partial p < 0$)

Impedance Parameter p	Frequency Interval†
b_{imp_m}	No frequency
k_{imp_s}	$\omega \in [0,\ \omega_{n_s}]$
b_{imp_s}	$\omega \in \left[\left(-\zeta_s + \sqrt{\zeta_s^2+1}\right)\omega_{n_s},\ \left(\zeta_s + \sqrt{\zeta_s^2+1}\right)\omega_{n_s}\right]$
m_{imp_s}	$\omega \in [\omega_{n_s}, \infty]$

† The frequency intervals are introduced in terms of $\omega_{n_s} = \sqrt{k_{imp_s}/m_{imp_s}}$ and $\zeta_s = b_{imp_s}/2\sqrt{m_{imp_s}k_{imp_s}}$.

Table 2 Parameters of control and adaptation laws used in experiments

Control Laws' parameters	Adaptation Laws' parameters
$\lambda_{2,m_1} = 1$, $\lambda_{2,m_1} = 1$,	$\mathbf{H}_{m_1} = 3.2I$,
$\lambda_{3,m_1} = 14$, $\lambda_{3,m_2} = 14$,	$\mathbf{H}_{m_2} = 3.2I$,
$\lambda_{3,s} = 115$, $\lambda_{4,s} = 1.6$	$\mathbf{H}_s = 24I$

Table 3 Parameters of impedance models (7) and (8) for the delay-free communication channels $T_1 = T_2 = 0$

Master impedance parameters	Slave impedance parameters	Force and position authority factors
$m_{imp_m} = 0.25$ kg $b_{imp_m} = 1$ N.s/m $\eta_f = 1/2$	$m_{imp_s} = 1.2$ kg $b_{imp_s} = 98$ N.s/m $k_{imp_s} = 4000$ N/m $\eta_x = 1$	Case 1: $\alpha_f = \alpha_x = 0.5$ Case 2: $\alpha_f = \alpha_x = 0.8$

Table 4 Modified impedance parameters for the absolute stability in the presence of communication delays (with the upper bounds of $T_1 = 70\ m\sec$ and $T_2 = 70\ m\sec$)

Master impedance parameters	Slave impedance parameters	Force and position authority factors
$m_{imp_m} = 0.25$ kg $b_{imp_m} = 18$ N.s/m $\eta_{\mathrm{f}} = 1/2$	$m_{imp_s} = 0.001$ kg $b_{imp_s} = 22$ N.s/m $k_{imp_s} = 350$ N/m $\eta_{\mathrm{x}} = 1$	Case 1: $\alpha_{\mathrm{f}} = \alpha_{\mathrm{x}} = 0.5$ Case 2: $\alpha_{\mathrm{f}} = \alpha_{\mathrm{x}} = 0.8$